RAPPORT SNO 5680-2008

Trace metal mobility and faunal effects of weight materials in water-based drilling muds

Sediment three months after addition of nine mm water-based cuttings (left) compared with control sediment with no addition (right).

Norwegian Institute for Water Research
– an institute in the Environmental Research Alliance of Norway

REPORT

Main Office
Gaustadalléen 21
N-0349 Oslo, Norway
Phone (47) 22 18 51 00
Telefax (47) 22 18 52 00
Internet: www.niva.no

Regional Office, Sørlandet
Televeien 3
N-4879 Grimstad, Norway
Phone (47) 37 29 50 55
Telefax (47) 37 04 45 13

Regional Office, Østlandet
Sandvikaveien 41
N-2312 Ottestad, Norway
Phone (47) 62 57 64 00
Telefax (47) 62 57 66 53

Regional Office, Vestlandet
P.O.Box 2026
N-5817 Bergen, Norway
Phone (47) 55 30 22 50
Telefax (47) 55 30 22 51

Akvaplan-NIVA A/S
N-9005 Tromsø, Norway
Phone (47) 77 68 52 80
Telefax (47) 77 68 05 09

Title	Serial No.	Date
Trace metal mobility and faunal effects of weight materials in water-based drilling muds	SNO 5680-2008	17.12.2008
	Report No. Sub-No. O-26152	Pages Price 54
Author(s) Morten Thorne Schaanning, Hilde Cecilie Trannum, Tor Fredrik Holth, Sigurd Øxnevad	Topic group FO	Distribution Open
	Geographical area	Printed NIVA

Client(s)	Client ref.
M-I SWACO	Siv Janne Aarrestad

Abstract

Ilmenite and barite minerals are alternative weight materials in water-based drilling muds for off-shore drilling operations. After use mud remnants may be discharged from the platforms and end up in cuttings deposits on the seabed. In order to assess potential environmental benefits from substitution of barite with ilmenite in drilling muds, a mesocosm experiment was performed in which 9 mm thick layers of various weight mineral and cuttings samples were added on the sediment surface of box core samples transferred from 35 m depth in the Oslofjord. One barite mineral sample was "markedly" contaminated with cadmium, copper, lead and zinc and the study showed increased release of the same metals to the overlying seawater. Slightly reduced number of species indicated that such elevated release of metals may harm sensitive macrobenthic species. The ilmenite mineral sample was "markedly" polluted with nickel and chromium, but only nickel was released to the overlying water at rates significantly higher than the release from control sediments and no effects on benthic organisms were observed in this treatment. All treatments with water-based cuttings showed oxygen depletion and lowered redox potentials within the sediment surface, and significant negative effects on the benthic communities. The release of metals were, however, lower in the cuttings treatments than in the mineral treatments as might be expected both from lower metal concentrations and the more reducing pore water conditions. The study has shown that substitution of contaminated barite with less contaminated barite or ilmenite may lead to less release of heavy metals such as cadmium, copper, lead and zinc from cuttings discharged off-shore. Increased discharge of ilmenite will however, increase the release of nickel to the off-shore environment.

4 keywords, Norwegian	4 keywords, English
1. Borekaks	1. Drilling mud
2. Marine sedimenter	2. Marine sediments
3. Utlekking metaller	3. Metal fluxes
4. Bunnfauna	4. Benthic fauna

Morten Schaanning
Prosjektleder

Kristoffer Næs
Research manager

Jarle Nygard
Strategy Director

ISBN 978-82-577-5415-0

Trace metal mobility and faunal effects of weight materials in water-based drilling muds

Preface

This report has been prepared for MI-SWACO in accordance with NIVA project proposal 14.03.05 and contract 11.07.2006. Box core samples were collected from RV Trygve Braarud, University of Oslo in April 2006. The experimental work was carried out at NIVAs Marine Research Station at Solbergstrand during the period October 2006 - January 2007. All chemical analyses were performed at NIVAs laboratory in Oslo. The test substances were supplied from MI-SWACO and arrived at NIVA in July 2006.

Oslo, 17.12.2008

Morten Thorne Schaanning

Contents

Summary

Objectives and experimental set-up
A mesocosm experiment has been performed at NIVA's Marine Research Station Solbergstrand situated by the Oslofjord outside the sill at Drøbak. The objective was to investigate the potential environmental benefits from substitution of barite with ilmenite in drilling muds. 0.1m^2 box-core liners with undisturbed benthic communities were transferred to the mesocosm from 35 m depth in Bjørnhodebukta, a small bay located a few kilometers north-west of the research station. 18 boxes were used for the 3 months experiment which started with addition of test substances on 05.oct. 2006 (=day 0) and finalised with analyses of the benthic fauna 08.-10.jan. 2007.

The boxes were treated with three different weight materials and two different types of cuttings sampled from off-shore drilling operation:

- BM1 = Barite minerals: moderately polluted with lead (Pb), cadmium (Cd), cupper (Cu) and zinc (Zn)
- BM2 = Barite minerals: markedly polluted with lead (Pb), cadmium (Cd) cupper (Cu) and zinc (Zn)
- IM = Ilmenite minerals: markedly polluted with nickel (Ni) and chromium (Cr),
- BC = Water-based cuttings with barite: moderately polluted with Pb, Ni, Cu and Cr
- IC = Water-based cuttings with ilmenite: moderately polluted with Zn, Ni, Cu and Cr.

All treatments were performed on three replicate boxes. In addition 3 boxes were left untreated for control (C).

Increased biodegradation in treatments with water-based cuttings
Chemical analyses showed that the cuttings contained significant amounts of organic carbon (TOC) and that the barite cuttings contained more (2.9%) than the ilmenite cuttings (2.0%). The weight materials contained <0.1% TOC. Several indications were found that degradable organic carbon stimulated the activity of heterotrophic bacteria in the sediment. Firstly, oxygen microelectrodes showed decreased downwards penetration of O_2 in cuttings treatments. Consistent with the higher concentration of TOC, this effect was larger in barite than in ilmenite treatments. Secondly, platinum electrodes showed decreased redox potentials in the cuttings treatments, and this effect was also more strongly developed in the barite treatments. Thirdly, the sulfide electrode gave clear evidence for increased sulphide ion activity in two of the eighteen experimental boxes, both of which had been treated with barite cuttings. Finally, the DGT probes (see below) showed increased amounts of reduced iron (FeII) and manganese (MnII) in the pore waters of the two cuttings treatments. The amount of Mn was larger in the barite cuttings than in ilmenite cuttings. Due to more sulphide production and precipitation of FeS, the amount of Fe was lower in the barite than in ilmenite treatments. Thus, various evidence was found on enhanced biodegradation of organic carbon in sediments treated with water-based cuttings and the stronger effect in barite compared to ilmenite cuttings was consistent with higher TOC in the added material.

In control (C) and mineral weight (IM, BM) treatments, O_2 penetrated down to 5-9 mm depth throughout the experimental period. In the cuttings treatments, however, O_2-penetration decreased to 1.9 mm in barite (BC) and 3.0 mm in ilmenite (IC) at the end of the experiment.

In control (C) and weight material (IM, BM) treatments the E_h decreased from more than 200 mV in the surface layer to 0-150 mV below 2-3 cm depth. In the cuttings treatments, E_h was -30-180 mV in the surface layer and -150-50 mV at 3-8 cm depth.

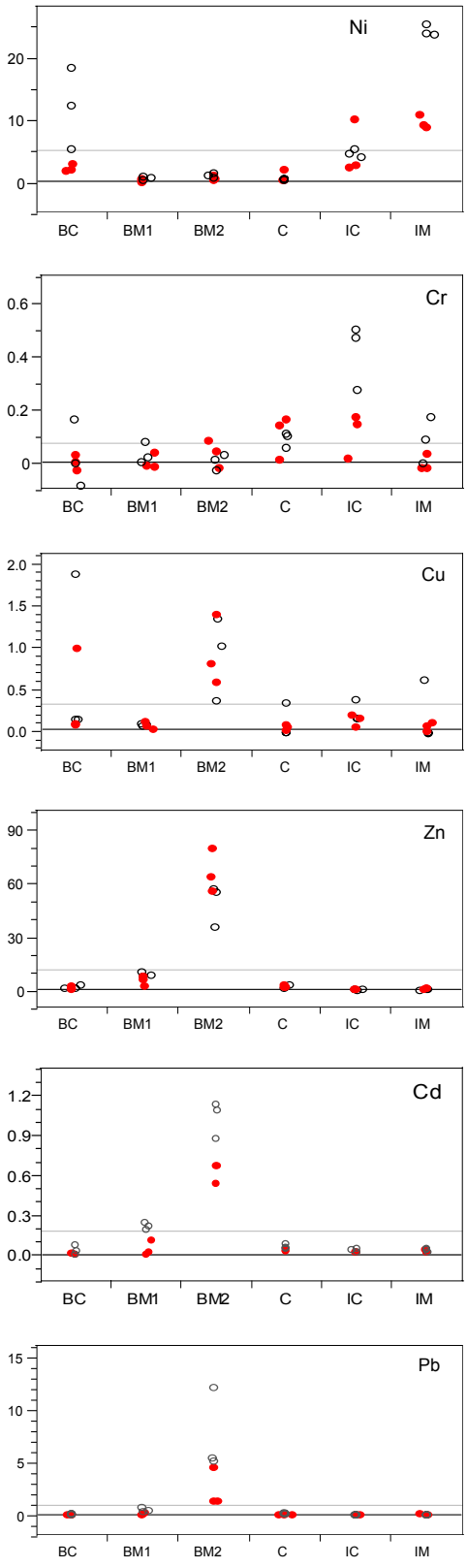

Fig. A. Metal fluxes (µg m^{-2} h^{-1}) from sediment to water. White symbols=first sampling. Red symbols=last sampling.

Metal fluxes

Metal fluxes (*Fig. A*) were determined from conventional water samples collected 41 and 91 days after addition of cuttings and on passive samplers exposed for the two periods day 11-41 and day 60-90. The passive samplers (DGTs) integrate the flux over the time of deployment and they only sample metal species which diffuse across the filter and diffusive gel, i.e. the most bioavailable fraction.

Statistical analyses showed that for lead (Pb), cadmium (Cd) and zinc (Zn), the release from the high-metal barite (BM2) was significantly higher than the release from all other treatments. Also, the release of cupper (Cu) was highest in BM2 and significantly higher than the flux of Cu from control sediments.

Nickel (Ni) and chromium (Cr) was often found to yield the highest fluxes in ilmenite treatments. Thus, Ni was released from ilmenite minerals (IM) at a rate of 16.8 µg m^{-2} h^{-1} which was significantly higher than the release of Ni from all other treatments. For chromium, the flux of 0.26 µg m^{-2} h^{-1} from ilmenite cuttings (IC) was significantly higher than all other treatments except control.

Sub-lethal biological effects

Biological effects of the various treatments were investigated by use of the CEA (Cellular Energy Allocation) method and by analyses of the macrobenthic communities remaining in the boxes after three months exposure to the test substances.

Analyses of CEA were performed using tissue samples from *Nuculoma tenuis* collected at the end of the experiment. The analyses revealed no difference between the various treatments. To some extent, this may have been due to decimation of the benthic community and insufficient amount of tissue sample for analyses in five of the six boxes treated with cuttings. None of the weight mineral treatments showed any evidence of sublethal effects as determined by the CEA method.

Macrobenthic community analyses

The macrobenthic communities remaining in each box at the end of the experimental period varied substantially (*Fig. B*). The number of individuals/box ranged from 4 to 95, the number of species/box varied from 1 to 19 and the Shannon Wiener diversity index from 0 to 3.4. Classified in accordance with criteria for Norwegian coastal and fjord waters, the benthic communities ranged from *class iii* (fair) or *class ii*

(good) in control and weight material treatments to *class iv* (bad) in ilmenite cuttings and *class v* (very bad) in two of the boxes treated with barite cuttings. Variance analyses (ANOVA) showed that both the number of individuals and the number of species were significantly less in the two cuttings treatments than in control and mineral weight material treatments. It was concluded that this was a redox or sulphide toxicity effect resulting from enhanced biodegradation of organic compounds present in the cuttings added.

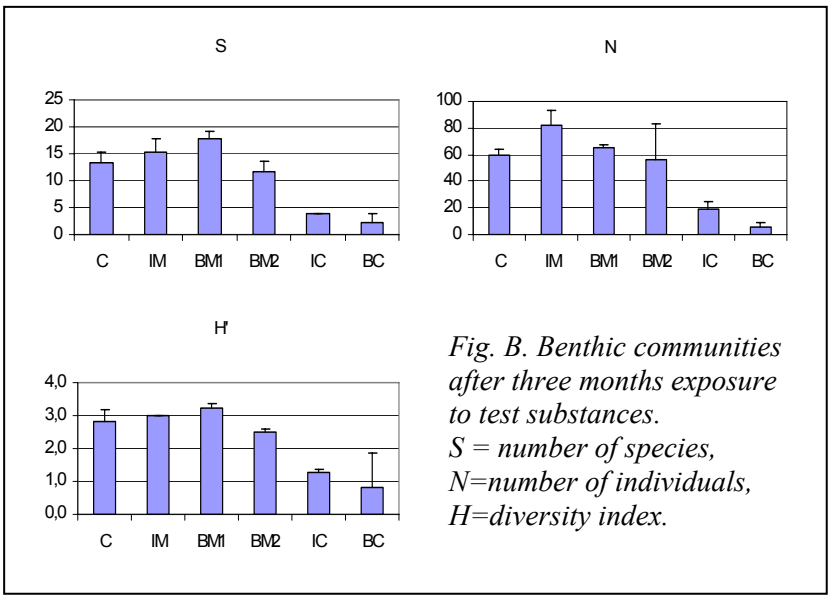

Fig. B. Benthic communities after three months exposure to test substances. S = number of species, N=number of individuals, H=diversity index.

The BM2 treatment ranked in between the cuttings and the other boxes, controls included (*Fig. B*). Thus, the number of species in BM2 was significantly less than in BM1 and significantly higher than in IC and BC. Any effect in BM2 would most likely result from increased exposure to heavy metals released from this type of barite. However, compared with control sediments and ilmenite weight materials, the observed deviations of community parameters in BM2 were not significant at the 95% level.

Environmental benefits of substitution of barite with ilmenite in drilling mud preparation

It has been argued that due to its lower content of heavy metals, ilmenite is an environmentally favourable barite substitute in drilling muds. Allthough this may not be true for nickel and chromium which was more abundant in the ilmenite sample than in both barite samples, this study confirmed that a shift to ilmenite based muds will reduce total discharges of cadmium, copper, lead, zinc and mercury. The study has also shown that substitution of the more contaminated barite with ilmenite or less contaminated barite, will reduce the release of heavy metals such as cadmium, copper, lead and zinc from off-shore cuttings discharges and hence reduce the amount of these metals available for uptake in marine organisms. Also, the mean release of mercury was less from ilmenite than from barite minerals, but these fluxes were small and not significantly different from zero. A shift towards increased discharge of ilmenite will, however, increase the release of nickel in the off-shore environment.

No significant difference was found between benthic communities exposed to barite or ilmenite minerals, neither when added as cuttings or as powdered mineral without any remnants of mud additives. However, a significant difference was found between the two barite minerals tested (BM1 and BM2). This appeared to be one of rather few reported evidence that metal release from mineral substances actually may affect the structure of benthic communities.

Biodegradable materials present in water-based cuttings may have a beneficial impact in reducing the release of metals from weight materials, but simultaneously enhanced biodegradation will have adverse redox or sulphide toxicity effects on the benthic community.

1. Background and objectives

Off-shore oil and gas activities currently accounts for approximately 1-3 % of total Norwegian discharges of cupper (Cu), lead (Pb), chromium (Cr), cadmium (Cd) and mercury (Hg) (table 1). Most of the metals discharged from offshore sources originate in weight materials in drilling muds and enters the sea associated with the cuttings produced in drilling operations. Barite is the most widely used weight material and discharge to the marine environment is permitted via its inclusion on the PLONOR list (OSPAR, 2002). Recent actions has, however, been taken to reconsider the presence on the PLONOR list of barite and alternative weight materials (Genesis, 2003).

Table 1. Discharge of heavy metals in Norway 2003. Total discharge and contribution from off-shore oil and gas activities. (Source: The Norwegian Pollution Control Authority - SFT, 2005).

	Cu	Pb	Cr	Cd	Hg
Total discharge	627	445	65	1.5	1
Off-shore industry	7	2.5	1	0.05	0.03

Barite ($BaSO_4$) is a naturally occurring mineral and the amount of heavy metal impurities may vary substantially in accordance with the actual ore from which it is mined. Alternative weight materials may be based on iron, manganese or titanium oxides, calcium or calcium-magnesium carbonates or strontium sulphate. Of these, the iron-titanium oxide mineral ilmenite appears to be the most frequently applied barite substitute. A systematic difference between the concentration of trace metal impurities in ilmenite and barite might have a significant impact on the discharge from the offshore industry. Considering the analyses of weight materials reported in Schaanning et al., 2002, substitution of barite with ilmenite would reduce discharges of Cu by 2-2.7x, Pb by 1.2-29x, Cd by 2-36x and Hg by 26-362x, and increase discharges of Cr (24-34x) and Ni (36-49x).

However, metal impurities in minerals are variously bound in lattice structures and other associations unavailable for uptake in marine organisms. Therefore, the environmental benefits from swapping weight materials depend primarily on the potential of their metal components to dissolve or desorb from the solid phase which is a prerequisite for accumulation in marine organisms.

In a previous work (Schaanning et al., 2002, Ruus et al., 2005), bioaccumulation of heavy metals in marine benthic species exposed to drilling mud weight materials was determined experimentally. The study gave clear and consistent evidence on elevated tissue concentrations of Ba in all organisms exposed to barite and Pb in organisms exposed to barites with the higher concentrations of this metal. In addition, some evidence was found for bioaccumulation of Hg and Cu, but lack of consistency between different treatments (different barite types) with similar exposure levels, left a need for further work to confirm or reject the potential for bioaccumulation of these metals. Another open question is whether the elevated concentrations of Ba were a result of particle transport across cell membranes (phagocytosis) or real uptake of dissolved, ionic species.

In the present study, the objective was to determine the release of trace metals from various weight materials and cuttings deposited on transplanted sediment communities. Simultaneously, the effects of the additions on the benthic communities were to be investigated in terms of full macrobenthic analyses of the sediment fauna by the end of the experimental period.

As a supplement to the classical community investigation, a new method was implemented to assess a general health status for a sediment-dwelling organism. The method is referred to as cellular energy allocation **(**CEA-analyses) and represents an equivalent to the physiological biomarker "scope for growth". The method involves measurement of total stored energy-equivalents (carbohydrate, lipid, protein) and total cellular respiration in the organism. Previous studies of another mollusc species, the zebra mussel (*Dreissena polymorpha*), have shown effects of chemical stressors in the CEA assay (Smolders et al. 2004, Voets et al. 2006). The available energy reserves have been shown to be a sensitive endpoint and to have a negative correlation to chemical stress. Of the available energy reserves, the lipid component have shown to be the most sensitive (Smolders et al., 2004).

2. Material and methods

2.1 Test set-up

2.1.1 Test substances

The choice of test substances was agreed upon at our meeting in Stavanger 10.03.06. The collection of test substances was organised by the contractor and delivered at NIVA's office in Oslo 11.07.06. As specified in Appendix A. the delivery contained five different materials:

- BM1 = Barite minerals type 1, pale yellow, dry powder
- BM2 = Barite minerals type 2, pale yellow, dry powder
- BC = Barite cuttings, grey, moist fine-grained sediment
- IM = Ilmenite minerals, black, dry powder
- IC = Ilmenite cuttings, dark grey, moist, fine-grained sediment

2.1.2 Field sampling, transfer and storage of test communities

From the research vessel RV Trygve Braarud, University of Oslo, box core samples were collected 06.04.06 at 35 m depth in Bjørnhodebukta, Oslofjord, SE Norway. The field site is located a few km to the north of the Marine Research Station at Solbergstrand. The samples were collected using a $0.1m^2$ KC-Denmark™ box corer modified with internal liners to retrieve undisturbed sediment samples (30 x 33 x 40 cm) in transparent polycarbonate boxes. The overlying water was removed through a siphon to reduce erosion of the sediment surface during transportation and handling. The boxes were covered with black plastic to avoid direct sun-light. Throughout sampling and transport the samples were maintained at the ambient temperature of 5-10°C both in air and sub-surface water.

In the mesocosm laboratory, 19 box core samples (18 for the experiment, one in reserve) were submersed in a tray continuously flushed with Oslofjord seawater from 60 m depth (OSW-60) supplied from the water inlet at this depth in the fjord adjacent to the research station. Air was pumped into each box through airstones positioned 1-2 cm above the sediment surface, and the overlying water exchanged freely with the tray water through holes in each box approximately 5 cm above the sediment surface. The boxes were covered with lids and left in the mesocosm with daily (working days) inspection until the experiment was ready to be initiated in October. Adaptation in the mesocosm environment for periods of 2-4 weeks is normally allowed before initiation of experiments. The main reason for this prolonged storage was delayed delivery of cuttings samples from off-shore drilling operations. However, maintenance problems were not encountered and no indications were found on increased mortality or reduced environmental quality during the pro-longed storage phase.

2.1.3 Experimental set-up

A few days before addition of test materials, the water exchange system was prepared for the experiment. All holes in the walls of the boxes were closed with silicon stoppers, and separate flows of 1-2 ml min^{-1} OSW-60 water was supplied to each box from an eighteen channel peristaltic pump through tubes (ID ≈ 2 mm) of PVC and marprene across pump rollers. Aeration and internal stirring was applied by an air-lift system in each box. This was done by mounting the airstones inside the open end of a transparent acrylic tube (ID ≈ 20 mm). The uplifted water was ejected horizontally in the upper part of the overlying water through holes in the tube shortly below the lid.

The test substances were added to the experimental boxes 05.10.06 (=day 0). Each of the five test substances were added to three replicate boxes. In addition, three boxes were left untreated for control. The actual treatment of each box was selected by random number generation, except that all three replicates were not allowed to occur in the same tray[1]. The result is shown in Figure 1. (The "C"-box to the lower left was not part of the experiment.)

Aliquots of each test substance (Table 2) was mixed with seawater and the resulting slurry was mixed into the overlying water from which the particles settled out to form even layers with a nominal thickness of approximately 9 mm. Up to eight days after addition, a slight turbidity revealed that a small fraction of the added particles remained suspended in the overlying water. Nevertheless, aeration, stirring and water exchange system was re-activated the day after addition and various settings of flow rates and aeration were applied, to force most of the fine fractions to sediment within the boxes and simultaneously maintain sufficient levels of O_2 in the water. After day 8 no further adjustments were made and the water flow was set at constant rate of about 2 ml min^{-1}. On day 11 the water was completely transparent. Although visible for a long period of time after addition, the fine fractions which were lost by wash out from the boxes will not account for more than a very small fraction of added particle mass.

Table 2. Addition of test substances and estimated layer thickness.

Treat-ment	Added test material (kg box^{-1})	Nominal layer thickness (mm)
C	0	0
BM1	1.00	9
BM2	1.00	9
BC	1.30	9
IM	1.00	9
IC	1.10	9

[1] The boxes in the two trays were assigned numbers from 1 to 19. For each treatment, random numbers between 0 and 99 were generated until three available numbers between 1 and 19 were obtained. If all three numbers occurred in one tray, new random numbers were generated until an available number in the other tray occurred.

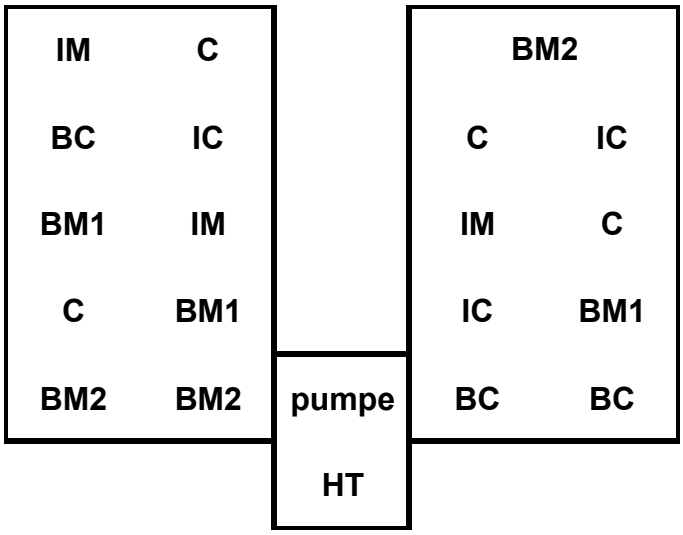

A.

B.

Figure 1. Overview of mesocosm set-up. A) Schematic B) Photo 06.10.06. NB! The control box to the lower left was not part of the experiment.

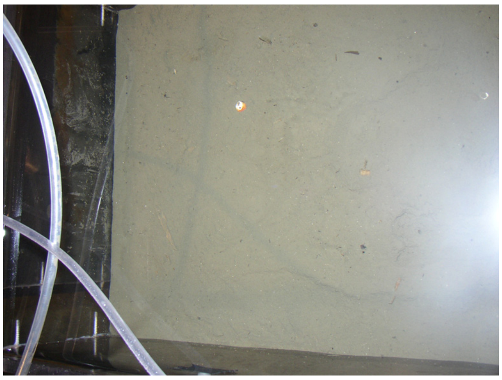

Control box 29.11.06.

Barite mineral treatment on 29.11.06.

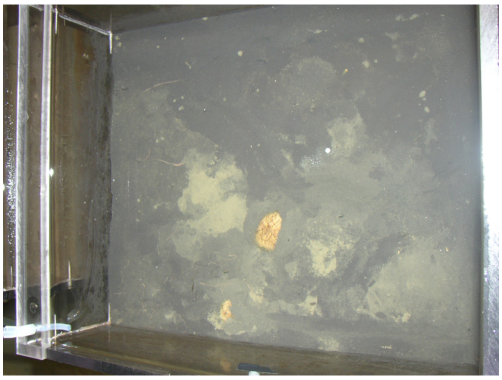

Ilmenite mineral treatment on 29.11.06.

Figure 2. Mixing between the added mineral materials and sediment provided by the sea urchin *Echinocardium cordatum*. Two partly buried individuals are shown in the middle-low of the picture of the ilmenite mineral treatment.

Table 3. Time schedule for sample collection (days).

Test substance added	0							
DGT water sampling		11	41		60	90		
DGT-probes pore water sampling						90-91		
Water samples for metals			41			90		
Pore water extraction for metals							93	
O2 microelectrode profiles	4			55			92	
Redox potential profiles							92	
Macrofauna and CEA sampling								95-97

2.1.4 Solid phase sampling and analyses

Solid phase samples were collected directly from the containers in which the various test samples were delivered and from the top 0-2 cm layer of the field zero samples.

Total concentration of metals in test substances and control sediments were determined after digestion in warm fluoric acid and analyses using ICP and ICP-MS for cadmium. Mercury was determined using gold trap extraction. The silt and clay fraction was determined gravimetrically after sifting the solid samples through a sieve with mesh-size 63 µm. Total organic carbon (TOC) was determined by combustion at 1800ºC in a Carlo-Erba 1106 element analyser after the removal of carbonates by acid leaching.

2.1.5 Water samples for flux measurements

Conventional samples for total trace metal analyses were drawn from the header tank and head space of each box on 15.11.06 (day 41) and 03.01.2007 (day 90). All bottles were prepared for metal analyses by pre-washing in dilute acid and sealed in double plastic bags before sample collection. Separate sample bottles were used for mercury (Hg) samples.

Titanium, barium, chromium, nickel, manganese and iron were determined by NIVA personnel using the HRICPMS (High Resolution ICP-MS) instrument at STAMI (Statens arbeidsmiljøinstitutt). Lead, cadmium and copper was determined at NIVA using freon-extraction and quantification in atomic absorption (AAS) with graphite furnace. Mercury was analysed using gold-trap extraction.

Fluxes were calculated from the equation:

$$\mathbf{F = (C_i - C_o)\cdot Q\cdot A^{-1}}$$

in which

F is the flux (µg $m^{-2}h^{-1}$)
C_i is the concentration in the headertank (µg L^{-1})
C_o is the concentration in the overlying water in each box (µg L^{-1})
Q is the flow of water through the respective box (L h^{-1})
A is the area of the core (m^{-2})

The flow of water across each core was measured gravimetrically after collection of outflow water for 4 minutes. The flow rate was determined 17.10, 15.11 and 02.01. The flow through each box ranged 1.50-2.05 g min^{-1} with a grand mean of 1.87 g min^{-1}. The variation (relative standard deviation) of the three repeated measurements in each box ranged 0.9-2.8%.

2.1.6 Passive metal samplers - DGT and DGT-probes

Passive metal samplers based on the thin-film gel (DGT) technique (Davison and Zhang, 1994, Røyset et al, 2002, 2003) yield time-integrated concentrations of the most bioavailable metal fractions. DGT-samplers for water-column sampling were deployed in the header tank and the head space water in each box. The first set of samples was deployed during the period 16.10. - 15.11.06 (day 11-41), and a second set was deployed for the period 04.12.06-03.01.07 (day 60-90). The DGT's were packed

individually in sealed plastic bags before deployment. After exposure, the DGT's were carefully rinsed with destilled water and stored in sealed plastic bags until analyses. Fluxes were calculated as described above (2.1.5).

The DGT probe (Davison et al., 1997) is a thin-film gel sampler designed for the study of trace metal mobility at the sediment water interface. After exposure of the probe in the sediment, the gel holding the ion-exchange resin (Chelex 100) is sectioned into thin slices. Each slice is eluted and metals determined using ICP-AES. DGT-probes for pore water sampling were deployed after the water samples had been drawn on day 90 (03.01.07) and exposed in the sediment for a period of 24 hours. The sampling window extended from 2 cm above the sediment-water interface to 13 cm below. After collection the probes were rinsed with distilled water and placed in sealed plastic bags. In the lab, the probes were sectioned in 5 mm slices down to 3 cm depth, then in 10 or 20 mm slices down to 12 cm depth.

2.1.7 Pore water

In addition to the DGT-probes, conventional pore water samples were collected from the 0-2 cm layer in all sediments. 5 cm (ID) core samples from each box were placed on a piston and the top 2 cm were pushed into a sectioning chamber and cut-off. The sectioning chamber was transferred to a N_2-tent within which the sediment slice was slipped into a plastic cup. The clay consistency allowed this transfer without breaking up the core slices. The sample cup was closed with snap lids and stored in plastic bags filled with N_2-gas until the next day when the sample was transferred to 50 ml tubes and pore water extracted by centrifugation at 12000 g for 30 min at 10 ºC. The supernatant was transferred to 25 ml vials using a pipette to avoid co-transfer of particles sticking to the walls of the tubes and analysed for total metal concentration as described above (2.1.5).

2.1.8 Oxygen microelectrode profiles and determination of oxic layer thickness

The oxygen saturation profile across the sediment-water interface was recorded on a Unisense™ Clark-type microelectrode (OX-50) with an internal reference and a guard cathode (Revsbech, 1989). The electrodes were connected to a picoammeter and output displayed on an online PC using Profix™ software, as shown in Figure 3. The measurements were performed in 10mm (ID) core sub-samples drawn from each box and mounted on a laboratory stand and a micromanipulator. Before measurements a two-point calibration was performed in well aerated and deoxygenated water. Microprofiles were determined in all box-core samples on on day 4, day 55 and day 92 after addition of cuttings.

O_2 saturation was recorded at 1 mm intervals from 5 mm above the sediment-water interface down to zero O_2 or maximum 20 mm sediment depth. Zero depth was assigned to the depth at which the O_2 concentration started to decrease relative to the constant readings always obtained through the water above the interface. The oxic layer was taken to be the distance between zero depth and the depth at which the interpolated oxygen saturation was 10%.

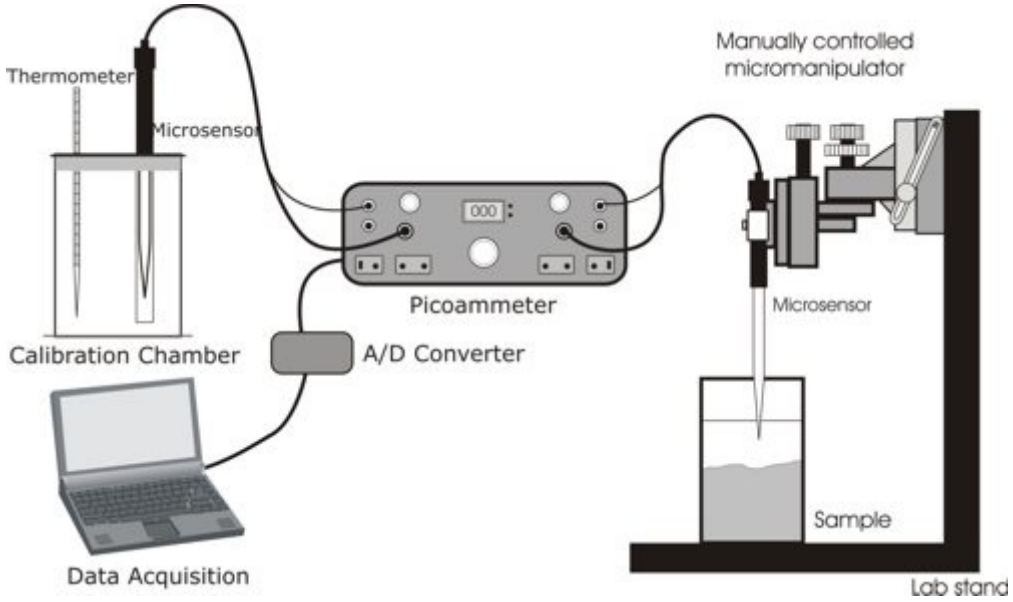

Figure 3. Microelectrode set-up.

2.1.9 Redox potential and hydrogen sulphide

Redox potentials and sulphide-ion activities were measured using, respectively, a conventional platinum electrode (Radiometer P101) and a Radiometer F1212S silver-silver-sulphide electrode. A silver-silver chloride reference electrode (Radiometer….) was used as common reference. The electrode assembly was controlled in a Zobell buffer solution before and after each series of measurements. The E_h was obtained by addition of the half-cell potential of the reference electrode (as specified by the manufacturer at 10 ^oC) to the in situ recorded rest potentials. Repeated measures of sediment samples had a precision better than ±10 mV at response times of one minute or less, but occasional slow response may provide larger errors in some measurements, in particular in samples measured close to redox discontinuity layers. The sulphide electrode is selective for the S^{2-} ions, and the concentration of hydrogen sulphide will depend on the pH in the sample which determines the relative concentrations of the three sulphide species H_2S, HS^- and S^{2-}. In this report, we merely report the potentials recorded on the electrode which will reveal the presence of sulphide in concentrations exceeding the detection limit for the electrode. At the pH normally found in marine sediments, the detection limit for $\sum H_2S$ is extremely low, i.e. at the nano-micro-molar level (Schaanning et al., 1997). Thus, if sulphide can be smelled in the sediment, it will be detected by the electrode.

Redox potentials and sulphide ion activities were measured during the core sampling on day 92. After retrieval from the box, the core was mounted on a stand and an assembly of conventional electrodes were inserted to depths of 5 mm and 15 mm (successively) below the sediment surface before cutting off the 0-2 cm section used for pore water extraction. After having removed the top section the electrodes were re-inserted to determine the potentials 5 mm below the cut-off sediment surface and at successive depths down to 7-8 cm (1 cm depth intervals).

2.1.10 Faunal analysis

By the end of the experiment (day 95-97), the sediment in each core was washed through a 1 mm sieve with round holes for macrofaunal analyses. The sieve residues were fixed in 10% buffered formalin, and stored in appropriate containers.

The macrofauna was sorted into main taxonomic groups (mollusca, polychaeta, crustacea, echinodermata and "varia") and preserved in 75-80% ethanol. The organisms were identified to species level or, where this proved difficult, to the lowest taxon possible. Biomass measurements (g wet weight) were performed for the main taxonomic groups.

Univariate measures for faunal data for each separate box and the fjord samples included total number of taxa (S), total abundance (N) and Shannon-Wiener diversity index calculated with $\log_2$ as the base. To analyse for similarities in the community structure, two multivariate analyses were performed based on the Bray-Curtis similarity measure: a cluster-analysis and MDS (multidimensional scaling). Similarity was calculated based on fourth-root transformed data. The calculation of the univariate parameters and the multivariate analyses were performed with the software program PRIMER (version 5.2.9) (PRIMER-E Ltd, 2002).

2.1.11 Cellular energy allocation

Overview

The protocol established at NIVA has been optimised and modified from that employed by De Coen & Janssen (1997). Samples were taken from selected species following exposure in sediment mesocosms. Therefore, the CEA assay was used to compare energy equivalents of exposed groups to a reference group, not as an integral of time.

The species present in the samples were used and for the current study this meant the sediment-dwelling bivalve *Nuculoma tenuis*. We hoped to find sufficient numbers of the polychaete *Polyphysia crassa*, but it was only present in three boxes. The organisms were carefully sieved from sediment and immediately frozen in liquid nitrogen. Samples were then stored at -80°C until analyses were performed. All work during the CEA assay was performed on ice unless otherwise noted.The analyses were performed on one mixed sample of the individuals collected from each box.

Homogenization

Samples were thawed, weighed and transferred to glass homogenisation tubes. Homogenisation buffer (0.4 M $MgSO_4$;15% polyvinylpyrrolidone (PVP);0.2% (w/v) Triton X-100 in 0.1M Tris buffer pH 7.5) was added equal to 3x the wet weight of the sample. The samples were then homogenized with Potter-Elvehjem glass/teflon homogenizer. Unhomogenised tissue was removed by brief centrifugation. Samples were stored in aliquots at -80°C until further analysis, except a small fraction immediately analysed for ETS-activity.

Activity of the Electron Transfer System (ETS)

ETS activity was determined as described by King & Packard (1975) with modifications by De Coen & Janssen (1997). Homogenized samples were combined in microtiter plates with Buffered Substrate Solution (BSS; 0.1M Tris buffer pH 7.5 containing 0.3% Triton X-100), NAD(P)H-solution (1.17 mM NADH, 250µM NADPH) and INT-solution (4 mg/ml 2-(p-iodophenyl)-3-(p-nitrophenyl)-5-phenyl tetrazolium chloride in distilled water). The change in absorbance was immediately measured at 490 nm at room temperature for 10 minutes. For converting the formed formazan to energetic equivalents conversion factors of 2 moles formazan: 1 mole O_2 and 484 kJ/mol O_2 were used (Gnaiger, 1983).

Measurement of lipid, protein and carbohydrate content

For converting measured values to energetic values, an enthalpy of combustion of 39,5 kJ g^{-1} for lipids, 24 kJ g^{-1} for proteins and 17,5 kJ g^{-1} for glycogen was used (Gnaiger, 1983).

Lipids

Total lipids were extracted following Bligh and Dyer (1959). The samples were mixed with chloroform, methanol and distilled water by vortexing and centrifuged at 14000 rpm for 5 minutes. 100 µl of the chloroform phase was added to a glass tube containing 500 µl concentrated H_2SO_4. A dilution series of tripalmitine (C16:0) in chloroform was used as standard. All preparations were then charred at 200°C for 15 minutes. Dilutions of charred samples were then transferred to microtiter plates and the total lipid content was quantified photometrically at 340 nm.

Proteins

Homogenates were analysed for total protein and lipid by the methods described in De Coen & Janssen (1997). Samples were added trichloroacetic acid (TCA, 15%) for protein denaturation. After brief centrifugation, the pellet was washed once with TCA (5%) and the supernatants combined for carbohydrate measurements.

The pellet was resuspended in NaOH (1M), incubated at 60°C for 30 minutes, then neutralized by adding HCl (1.67M). Protein was determined as described by Lowry et al. (1951) adapted for plate reader.

Carbohydrates

Samples were incubated in microtiter plates with H_2SO_4 and phenol (5%) in room temperature for 30 minutes. The absorbance was then measured at 490 nm. A dilution series of glycogen was used as standard.

Test organism

The species selected for the CEA-analyses was a subsurface deposit-feeder *Nuculoma tenuis* Montagu. This organism is a typical isomyerian bivalve in which the flow of water is from both anterior and posterior directions. It is common in sediment from the sublittoral zone to abyssal depth (Harvey and Gage 1995). Its feeding activities usually generate disturbance in the top two or three cm of the sediment (Widdicombe and Austen 1999) and hence unlikely to avoid interaction with the added substances.

3. Results and discussion

3.1 Test substance analyses

Fine fraction and organic carbon is shown in Table 4.

Of the mineral samples (IM, BM1 and BM2) 95-99% of the particles was in the <63µm size fraction, as compared to 35 and 58% in the two cuttings samples and 78% in the control sediment.

Organic carbon was not detected (<0.1%) in the mineral samples. The cuttings contained respectively, 2.02 and 2.90% TOC as compared to 3.18% in the control sediment.

Table 4. Particle size fraction <63µm and total organic carbon (TOC) in control sediment (C) and added materials. IM=ilmenite mineral, BM = barite minerals type 1 and 2, IC = ilmenite cuttings, BC = barite cuttings.

	Size<63µm	TOC
Treatment	% of dry weight	
C	78	3.18
IM	99	<0.1
BM1	95	<0.1
BM2	99	<0.1
IC	58	2.02
BC	35	2.90

Table 5. Metal concentrations (µg g^{-1} d.wght.) in control sediment and added materials in present and previous experiments. Colours indicate contaminant level in accordance with Norwegian quality criteria for coastal and fjord sediments: blue for class I "insignificantly polluted", green for class II "moderately polluted" and yellow for class III "markedly polluted" (after Molvær et al, 1997).

	Ba	Ti	Cd	Cr	Cu	Hg	Ni	Pb	Zn
Control									
C	507	2360	0.182	8	43	0.380	41	70	150
Ilmenite									
IM	7	265000	0.032	466	32	0.005	145	3	66
Previous[1]	1500	252000	0.03	469	38	0.005	147	8	100
Barite									
BM1	10600	68	0.407	21	74	0.032	3	89	130
BM2	10900	40	1.93	27	159	0.076	5	245	705
Previous[2]	9220	na	0.77	18	100	0.370	4	130	197
Cuttings									
IC	2900	44500	0.253	155	54	0.033	70	10	160
BC	7340	3850	0.828	79	67	0.037	61	36	97

[1]Ilmenite and [2]barite (Zelmou/Safi) mineral samples analysed with the same method of mineral digestion (Schaanning et al., 2002).

As expected, the metal analyses (Table 5) confirmed high concentrations of barium (Ba) in barite mineral and cuttings samples and high titanium concentrations in ilmenite mineral and cuttings samples. One of the barite minerals (BM2) had class III concentrations (markedly polluted) of cadmium, copper, lead and zinc, whereas the ilmenite mineral (IM) had class III concentrations of chromium and nickel. Neither of the two cuttings samples (IC and BC) exceeded class II "moderately polluted" with respect to any metal, but several metals were more abundant in the cuttings samples than in the "mother" mineral phases.

The comparison with the samples of the weight material used in a previous experiment (Schaanning et al, 2002) shows that, except for barium, the two ilmenite samples were very similar. (Barium is difficult to extract reproducibly from the solid phase, and severe analytical errors may account for the difference between the two ilmenite samples shown in Table 5). Compared with the previous barite sample, BM1 was lower and BM2 was higher with respect to the concentration of most trace metals. The exception was Hg which was low in both current samples compared to the previous sample.

Unfortunately, the control sediment was moderately polluted with respect to all of the analysed trace metals and the concentration of Hg was higher in the control sediment than in any of the test materials. Ideally, control samples should not exceed background levels with respect to any contaminants addressed in the experiment. The control station has been used for many previous experiments and was chosen because of the well documented benthic fauna.

3.2 Test environment

3.2.1 Oxygen profiles

Because of the continuous aeration of the overlying water, the O_2-saturation was maintained close to 100% in all boxes throughout the experimental period. At the sediment surface the saturation dropped sharply (Figure 4) and crossed over the 10% saturation level at depths between 1.7 and 12.6 mm. In control boxes and the three mineral treatments (IM, BM1 and BM2), the thickness of the oxic layer showed no clear change with time and no differences were found between treatments and control.

In the two cuttings treatments, however, the oxic layer decreased with time (Figure 5). This was confirmed by the variance analyses shown in Table 6. This analyses (ANOVA, Tukey comparison of all pairs) was run for each series of measurements and for all series pooled. The results are displayed by letters assigned to each treatment (level). If two levels are not connected by the same letter, the two levels are significantly different at the 95% significance level.

Thus, on day 4, all levels were assigned the same letter (A) which means no significant difference between treatments. On day 55, the two cuttings treatments IC (mean oxycline=3.9 mm) and BC (3.2 mm) was significantly smaller than the mineral treatment BM1 (9.0 mm), but not different from control C (5.8 mm). However, during the final sampling, the two cuttings treatments were significantly lower than control C and BM2. For the whole experiment (n=54), BC was significantly less than BM1, BM2 and C whereas IC was significantly less than BM2, only.

3.2.2 O_2 discussion

The penetration of O_2 into the sediment results from the balance between chemical and biological consumption in the sediment and supply from the overlying water by diffusion and bioturbation (vertical mixing of sediment and pore water, irrigation of tubes and cavities). Assuming that physical variations are small between current treatments and that bioturbation varies at random, variations in the depth of the oxic layer will primarily result from variations in the rate of O_2 consumption. If the

chemical and biological oxygen consumption represent the sum of the major anaerobic and aerobic biodegradation processes, the reduced layer thickness in the cuttings treatments most likely results from biodegradation of some organic phase present in the water based cuttings.

An alternative explanation might be increased mortality and decay of dead organisms. However, the accute toxicity of water-based cuttings should be low and most of the biomass in these sediments is normally accounted for by a few large individuals (c.f. Schaanning et al., 2007, and Figure 24 below). In contrast to a homogenously distributed organic component of the cuttings, such organisms would, post-mortem, provide small spots with high rates of O_2 consumption and little change over most of the sediment surface. Such spots would rarely be sampled at random and if visually different from the rest of the sediment surface, such areas would not have been sampled at all. (The core samples drawn for electrode measurements were always drawn form areas which appeared representative for the whole box.)

The maximum biomass in each box was 20-30 g wet wght. (Figure 24). This corresponds to about 3-6 g TOC. The fact that 20-30 g TOC was added with the cuttings (estimated from data in Table 2 and Table 4) suggested that the cuttings would be a more important source of degradable organic carbon than dead macrofauna. The 3.18% TOC present in control sediment will be mostly old, refractory carbon phases which contribute little to SOC. Comparison of the two cuttings treatments showed that the lower OLT (2.7 mm) and higher TOC (2.90%) in the barite cuttings was consistent with the higher OLT (4.6 mm) and lower TOC (2.02%) in the ilmenite cuttings. It seems, therefore, that rather than accute toxicity followed by decay of dead organisms, the decreased OLT in the cuttings treatments was a direct result of biodegradation of TOC added with the cuttings.

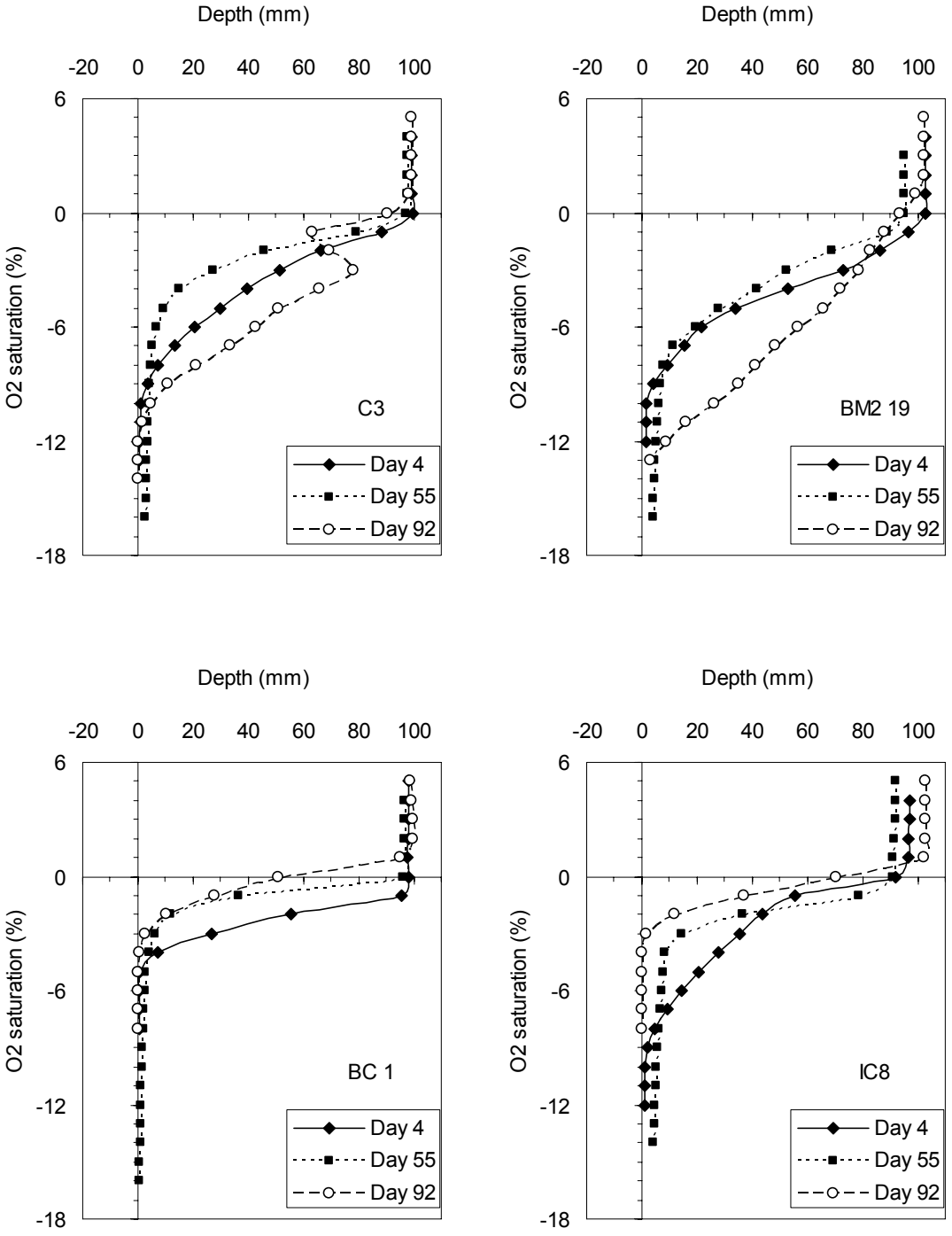

Figure 4. Typical microelectrode profiles of oxygen saturation in untreated control box (C 3), and boxes treated with barite minerals (BM2 19), barite cuttings (BC 1) and ilmenite cuttings (IC 8).

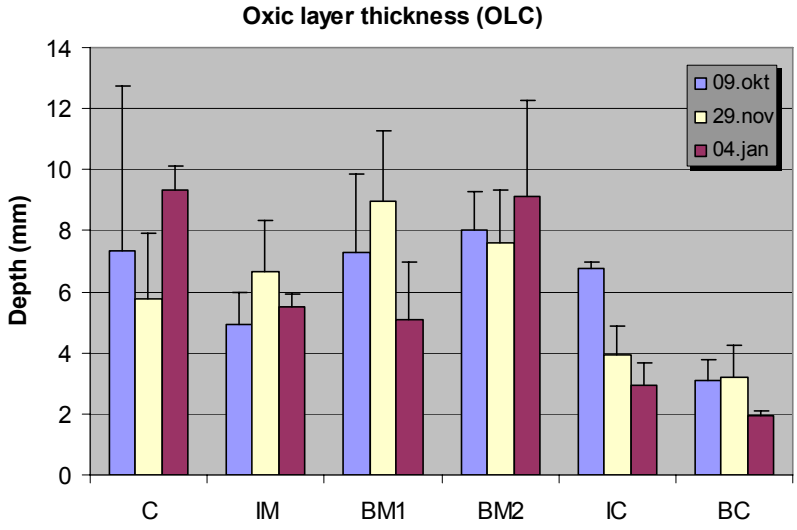

Figure 5. Distance from sediment-water interface (100% O_2 saturation) to depth at which oxygen concentration is <10% saturation. Average and 1 standard deviation of the three replicate boxes of each treatment.

Table 6. Results of variance analyses (ANOVA, Tukey comparison) of oxygen layer thickness (mm) for each and for all surveys (see text).

Day 4 (n=18)			Day 55 (n=18)				Day 92 (n=18)				All days (n=54)				
Level		Mean	Level			Mean	Level			Mean	Level				Mean
BM2	A	8.0	BM1	A		9.0	C	A		9.3	BM2	A			8.2
C	A	7.3	BM2	A	B	7.6	BM2	A		9.1	C	A	B		7.5
BM1	A	7.3	IM	A	B	6.6	IM	A	B	5.5	BM1	A	B		7.1
IC	A	6.7	C	A	B	5.8	BM1	A	B	5.1	IM	A	B	C	5.7
IM	A	4.9	IC		B	3.9	IC		B	3.0	IC		B	C	4.6
BC	A	3.1	BC		B	3.2	BC		B	1.9	BC			C	2.7

3.2.3 Redox and sulphide electrode potentials

Vertical profiles of redox potentials (E_h) are shown in Figure 6. The figure shows that in control and mineral treatments the E_h decreased from 200-250mV in the surface layer (0-2 cm) and decreased with depth to 0-150 mV below 3 cm. In the two cuttings treatments, the Eh was down to 0-50 mV within the surface layer. Below 3 cm, the ilmenite cuttings treatment (IC) was only slightly lower than control and mineral treatments, whereas the barite cuttings treatment had decreased to values between -50 and -200 mV.

Slow electrode response showed that hydrogen sulphide was present in low concentrations in the pore water in most of the boxes of this experiment. In such a series of measurements, each value recorded is partly dependent on the preceding measurement and the presence of sulphide is revealed as a sudden decrease of the Es. Therefore, only the two BC-treatments BC 9 and BC 16 provided clear evidence

for the presence of H_2S (Figure 6). Possibly, also the drop of Es in IC-4 and BM2-5 may indicate som S^{2-}activity. The fact that no indications on S^{2-} were found in BC-1 was confirmed by the E_h which was >-1mV throughout this core, as compared to <-107 mV below 5 cm depth in BC-9 and BC-16.

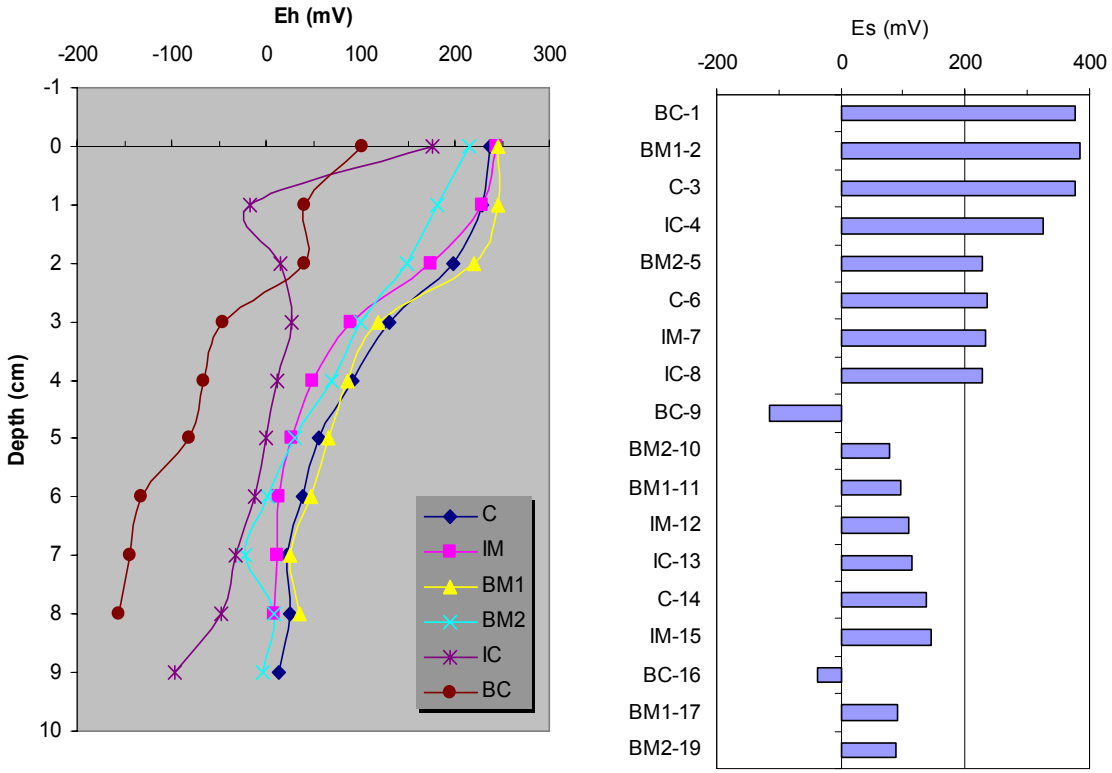

Figure 6. Redox (Eh) and sulphide (Es) potentials, final sampling 05.01.07. Left: mean Eh profiles for each treatment. Right: Es in each box measured successively from top (BC-1) to bottom (BM2-19).

3.2.4 Discussion E_h and E_s

Biodegradable organic carbon in sediments will be oxidised by bacteria utilising available O_2 and subsequently other electron acceptors such as NO_3, Mn(IV), Fe(III) and more abundant SO_4^{2-}. The Pt-electrode may respond to increased concentrations of iron and manganese, frequently providing an E_h of about 0-100 mV (Bågander og Niemistö, 1978). The sulphide electrode, however, only responds to S^{2-}-ions. Sulphide produced by sulphate reducing bacteria (SRB) will be consumed by precipitation of metal sulphides. Therefore, sulphide may not be detectable in sediments even though SRB's are actively involved in carbon oxidation. Not until the metal buffers have been depleted, or the rate of sulphate reduction is faster than sulphide precipitation, the activity of S^{2-} becomes detectable. If the carbon is slowly degradable, or the carbon source becomes depleted before this point is reached, sulphide may never proliferate to detectable levels. Thus, it appears that only BC-9 and BC-16 had proceeded to sulphide accumulation in the pore water. BC-1 and the three IC-boxes appeared to be in an intermediate state at which sulphide was still below detection limits, but where increased activities of Fe^{2+} and Mn^{2+} ions had lowered the E_h relative to control and mineral treatments. Again, the

difference between the IC and the BC treatment was consistent with the lower concentration of TOC in the ilmenite cuttings (Table 4 and section 3.2.2).

The photographs of the cores taken immediately before the electrode measurements (Figure 7) showed that the control sediment was grey with little visible layering. The layer of black ilmenite minerals (top right) covered only the uppermost cm of the sediment, but smearing masked the appearance of grey sediments below the top layer. In the barite cuttings treatments BC-9 and BC-16, the precipitation of black ferrous sulphide (FeS) is seen to occurr below ca 5 cm depth in which both electrodes displayed low potentials.

BC-9 and BC-16 were the only cores in which black sediments not related to black ilmenite minerals, were observed. Similar to C-14 in Figure 7, the other cores were grey with distinct surface layers which were either pale yellow due to barite minerals or black due to ilmenite minerals.

Figure 7. Core samples 05.01.07. Top left: barite cuttings (box 9), top right: ilmenite mineral (box 12), lower left: control (box 14), lower right: barite cuttings (box 16). Thickness of added layer is clearly seen in top left core

3.3 Metals

3.3.1 Pore water concentrations

The correlation between concentration of metals in pore water and solid phase was investigated by simple linear regression analyses of the metal concentrations in the pore water extracted from the top 0-2 cm layer of the sediment and the concentration in the solid phase of the materials added and of the top 0-2 cm of the control sediment. The result is shown in Table 7 and plot examples are shown in Figure 8.

Pb, Ni and Zn displayed good correlations ($0.65<R^2<0.72$) between the concentrations in solid phase and pore water.

Ba, Cd and Hg showed a significant ($p<0.05$) increase of pore water concentration with increased solid phase concentration, but the correlation was poor ($0.18<R^2<0.42$).

Ti, Cr and Cu did not show any significant increase with increasing solid phase concentrations ($p>0.05$) in spite of large differences between low and high solid phase concentrations; i.e. 5000x for Ti, 60x for Cr and 5x for Cu.

Table 7. Results of linear regression analyses of metal concentration in pore water extracted from 0-2 cm of the sediments vs concentration of metals in solid phase of control sediment and added materials. Data plots are shown in Figure 9.

C_{pw} ($\mu g\ L^{-1}$)		intercept		slope	C_{sed} ($\mu g\ g^{-1}$)	R^2	p	n
Pb_{pw}	=	1.24	+	0.0178	Pb_{sed}	0.7167	<.0001	18
Ni_{pw}	=	1.05	+	0.0687	Ni_{sed}	0.6867	<.0001	18
Zn_{pw}	=	7.83	+	0.0649	Zn_{sed}	0.6505	<.0001	18
Cd_{pw}	=	0.0094	+	0.2143	Cd_{sed}	0.4161	0.0023	18
Ba_{pw}	=	11.52	+	0.0139	Ba_{sed}	0.2759	0.0147	18
Hg_{pw}	=	0.017	+	0.0562	Hg_{sed}	0.1859	0.0421	18
Ti_{pw}	=	4.59	+	0.00001	Ti_{sed}	0.0435	0.2017	18
Cr_{pw}	=	0.75	-	0.0002	Cr_{sed}	-0.0582	0.8009	18
Cu_{pw}	=	10.64	-	0.0028	Cu_{sed}	-0.0597	0.8406	18

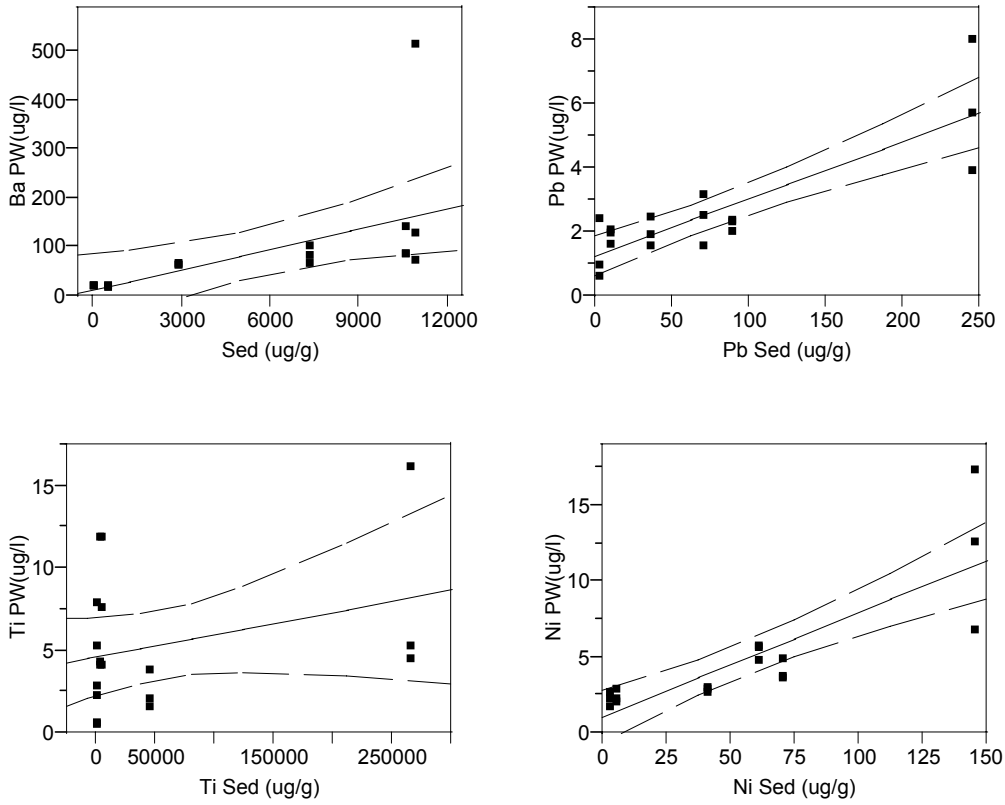

Figure 9. Best fit linear curves and 95% confidence intervals for metals in pore water vs metals in solid phase of control sediment and added materials. Curve equations are given in Table 7.

3.3.2 DGT-probes

Vertical profiles of the uptake of metals on DGT-probes exposed at the sediment-water interface for 24 h during day 90-91, are shown in Figure 10-Figure 12. Fe and Mn showed high uptake rates in the 0-7 cm layer of the cuttings treatments. A large peak of Fe occurred in IC (box 4) and a large peak of Mn occurred in BC (box 9). Because other metals may interact with dissolution/precipitation of Fe and Mn, the total uptake in the 0-7 cm during the 24h deployment period was calculated. The total uptake is shown in Table 8 and total uptake in excess of uptake in control is shown in Figure 13.

In BC-9, the gradient of Mn-uptake extended into the overlying water. This indicated leakage of mangenese from the sediment to the overlying water in this box. Similarly, the DGT-profiles gave clear evidence on leakage of Pb, Zn and Cd from BC-9.

At 2-3 cm depth a slight increase of Mn uptake rates in control sediments and mineral treatments (Figure 10, box C, BM1, BM2, and IM) revealed the depth of the redox boundary for Mn(IV)/Mn(II) minerals. Similarly, the redox boundary for Fe(III)/Fe(II) minerals was revealed by increased Fe uptake rates at 5-6 cm depth. Compared with the Eh in Figure 6, the Mn redox-boundary co-occurred with the redox-cline at about 250 to 100 mV, whereas the Fe redox boundary occurred at slightly lower Eh (100-0 mV), and without any clear interaction with the vertical profile of Eh. The upwards migration of the Fe- and Mn-redox-boundaries in the cuttings treatments had a large impact on Fe- and Mn-profiles. Because of the frequent adsorption/desorption of other metals on the surface of Fe- and Mn-minerals, the dislocation of Fe- and Mn-redox reactions is an important factor which may affect the distribution of other metals as well.

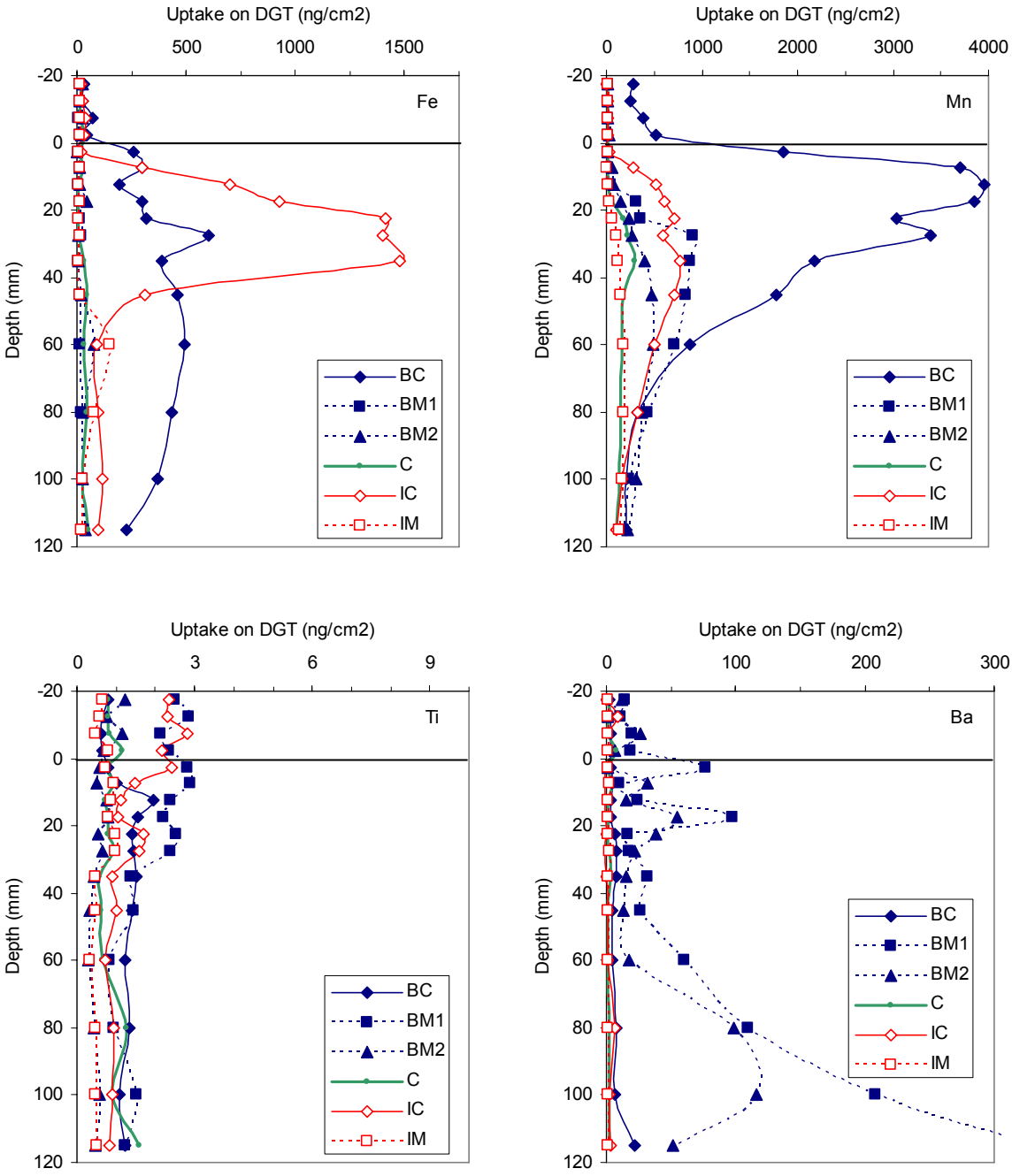

Figure 10. 24 hours DGT-uptake profiles of Fe, Mn, Ti and Ba in one box from each treatment determined on day 90-91.

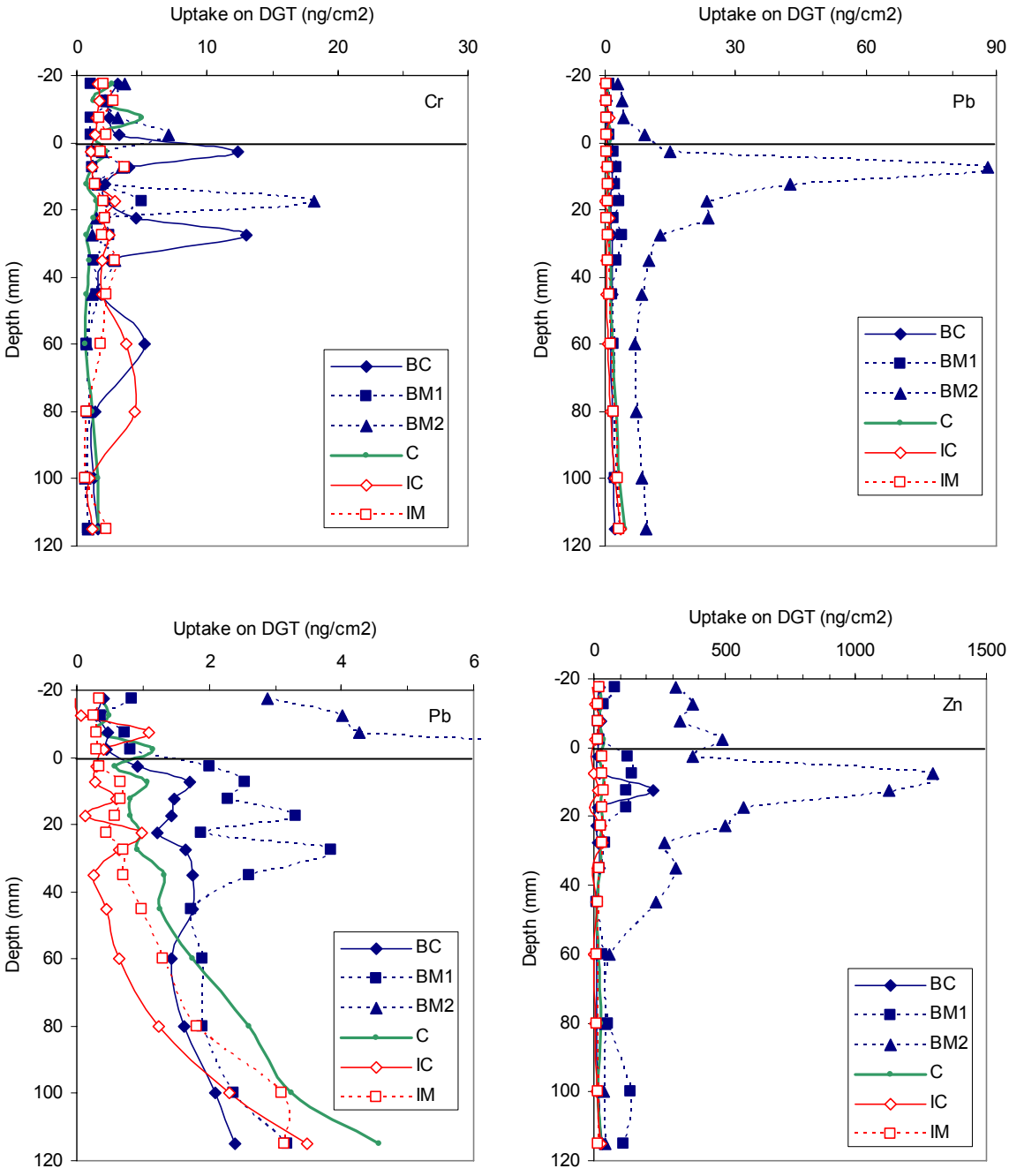

Figure 11. 24 hours DGT-uptake profiles of Cr, Pb (scale 90 ng/cm^2 and 6 ng/cm^2) and Zn in one box from each treatment determined on day 90-91.

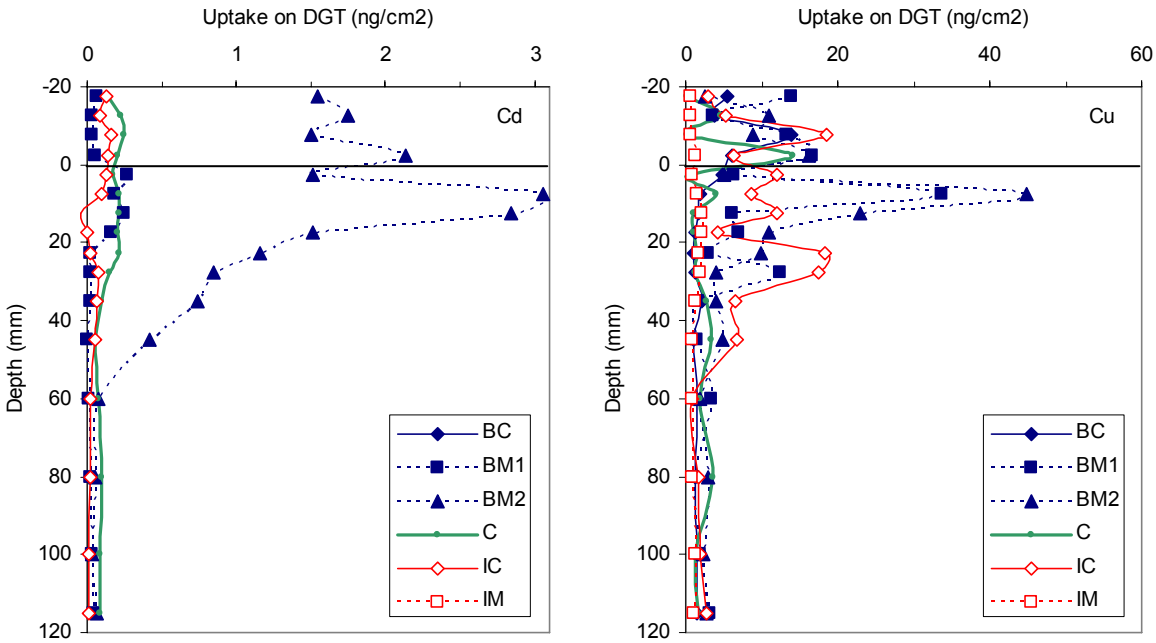

Figure 12. 24 hours DGT-uptake profiles of Cr, Pb (scale 90 ng/cm^2 and 6 ng/cm^2) and Zn in one box from each treatment determined on day 90-91.

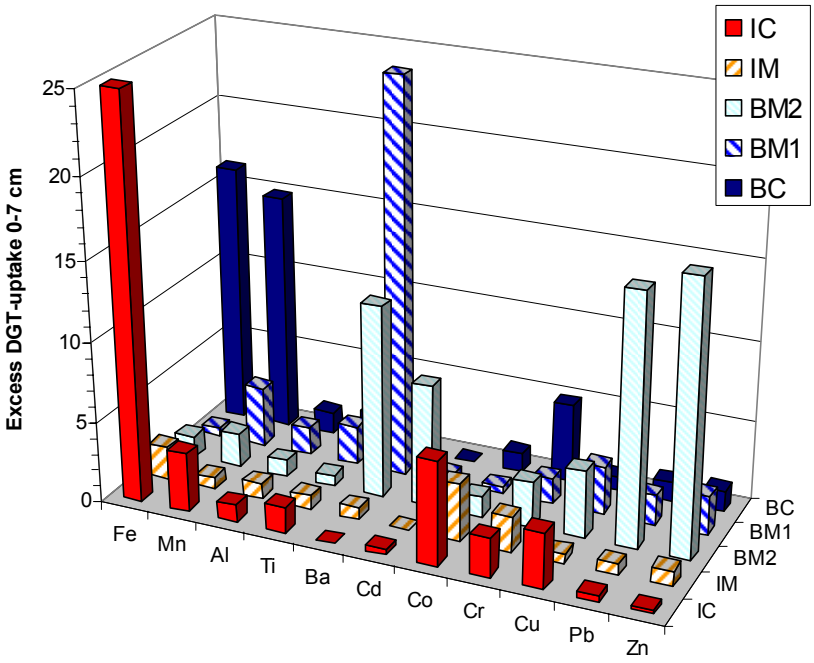

Figure 13. Total 24h DGT-uptake in 0-7 cm layer in each treatment normalised to control (ng).

Table 8. Total 24h DGT-uptake in 0-7 cm layer in each treatment normalised to control (ng).

	Al	Ti	Ba	Fe	Mn	Cd	Cr	Cu	Pb	Zn	V	Mo
IC	1.10	1.63	0.01	25.15	3.69	0.34	2.46	3.50	0.40	0.21	0.61	0.19
IM	0.97	0.86	0.73	2.07	0.71	0.00	2.22	0.60	0.69	0.96	0.80	0.73
BM2	1.02	0.66	11.97	1.31	2.13	7.63	2.84	4.22	15.66	16.9	0.71	0.82
BM1	1.72	2.44	24.68	0.51	3.76	0.56	1.61	3.01	1.86	2.49	0.33	0.52
BC	1.38	1.92	2.90	16.27	14.8	0.00	4.90	0.84	1.22	1.31	0.88	0.54

The vertical profiles of Ti and Ba (Figure 10) showed no clear patterns, but the total uptake of Ba in the 0-7 cm layer was 2.9-24.7x higher in the barite treatments than in control as compared to the ilmenite treatments in which uptake rates were less than control (Table 8). It might have been expected that Ti would have shown a similar distribution with higher uptake in IC and IM than in control and barite treatments, but the data provided no evidence to support this.

The uptake of Cr within the 0-7 cm layer was 1.6-4.9x higher than control in all treatments. The uptake of Cu was higher than control in IC, BM2 and BM1, but lower in BC and IC. Thus, the DGT-data for Cu and Cr appeared to confirm the lack of systematic variation in the pore water found in Table 7.

Both BM treatments showed clear peaks of Cu-uptake 5-10 mm below the sediment surface (Figure 12). At this depth, BM2 provided high uptake rates for Pb, Cd and Zn. Undoubtedly, these peaks result from dissolution or desorption of metals from the BM2 weight material. Elevated Pb uptake rates were also observed in BM1 (1.9x control) and BC (1.2x control), but the vertical profiles (Figure 11) indicated two separate sources for Pb, one near the surface and another one below the redox cline at 2-3 cm depth. Desorption of Pb during reduction and dissolution of Fe- and/or Mn-oxides is the most likely process to explain the secondary deep source of Pb. Also Zn showed elevated uptake rates in BM1 (2.5x control) and BC (1.3x control), most of which occurred at 0-2 cm depth, within or near the layers of added barite weight materials and cuttings.

Conclusively, the DGT-profiles gave clear evidence that the added BM2 weight material was a source for dissolution of Zn, Pb and Cd. It also appeared that both BM1 and BM2 represented a source for dissolution of Cu.

3.3.3 Metal fluxes

Instantaneous fluxes of total metals were determined from discrete water samples taken on day 41 and 90 and analysed for total metals. In addition, time-integrated fluxes of the metal fractions available for uptake on DGTs were determined for two periods of 30 days exposure (day 11-41 and 60-90). All flux measurements are shown in Figure 14-Figure 18.

Fe-fluxes varied about zero in most of the treatments. The DGT samples revealed no difference between any treatments. BM1 showed a mean release of 0.4 µgFe m-2 h-1, but strongly influenced of one outlier measurement.

Consistent with the DGT-profile shown in Figure 10, Mn-fluxes were close to zero for all treatments except BC. In this treatment, the time integrated samples gave a mean flux of 65 µg m^{-2} h^{-1}, which was significantly higher (α=0.05) than all other treatments and control. The time integrated samples also shows that elevated fluxes occurred in only two of the three replicate boxes and that the fluxes during the second sampling period were less than the fluxes during the first sampling were lower The discrete water samples showed high fluxes (2250 µg m^{-2} h^{-1}) in two of the boxes on day 41, but low fluxes in

the third box and in all boxes sampled on day 90. Clearly, the release of Mn was highest during the first part of the experiment and decreased towards the end.

In most cases, Ti was taken up from water to sediment. Thus, the mean flux was negative in all treatments. A positive flux was observed in control, only. The release of Mn from the control sediment was significantly different from the uptake in BC, only (Figure 15). Thus, neither DGT-probes nor flux measurements gave any evidence for release of Ti from ilmenite minerals in weight materials or cuttings. This was consistent with the lack of correlation between Ti in sediment and conventional pore water samples shown in Figure 9 and Table 7.

Barium was released from all sediments, but the fluxes from the barite treatments BC and BM2 were significantly higher than the release of Ba from control sediment (Figure 15). Allthough the internal ranking between the barite treatments were different, this was consistent with elevated DGT-uptake rate from pore water (Table 8) and the significant ($p<0.05$) relationship between sediment and conventional pore water samples shown in Table 7.

Mercury was also released from all sediments. The highest release (1.0-1.2 $\mu g\ m^{-2}\ h^{-1}$) occurred in BM1, BM2 and control. The lowest release was observed from IM. To some extent this was consistent with the fact that control sediment had the highest and IM had the lowest concentration of Hg, and that, allthough poor, a significant correlation was found between Hg in sediment and pore water (Table 7). Significant differences between any treatments were not found for Hg fluxes.

Neither DGT water samples nor the DGT-probes provided any conclusive data on Cr. Possibly the DGT-technique is not suitable for the study of this element in seawater media. The discrete water samples showed the highest flux of Cr from the ilmenite cuttings (0.26 $\mu g\ m^{-2}\ h^{-1}$) and this flux was significantly higher than the release from IM and all barite treatments. Thus, even though the ilmenite weight material had a concentration of 466 $\mu gCr\ g^{-1}$ d.wght. (Table 5) compared to 155 $\mu g\ Cr\ g^{-1}$ d.wght. in the cuttings, more Cr was released from the cuttings.

Nickel was released from the ilmenite weight materials at rates significantly higher than the release from any other treatments, control included (Figure 16). This was consistent with the high solid phase concentration of Ni in ilmenite weight material (Table 5) and the close correlation between solid phase and pore water concentrations shown for this element (Table 7). The cuttings samples had intermediate levels of Ni in the solid phase and Ni release of 1.1-7.0 $\mu g\ m^{-2}\ h^{-1}$ was intermediate between 7.8-16.8 $\mu g\ m^{-2}\ h^{-1}$ in IM and the low rates 0.04-0.75 $\mu g\ m^{-2}\ h^{-1}$ observed in C, BM1 and BM2.

For Pb, Zn, Cd and Cu, the highest release always occurred from BM2 and the release from this treatment was always significantly higher than the release from control sediments (Figure 17, Figure 18). Next to BM2 the highest release of Pb, Zn and Cd occurred in BM1, whereas the next highest flux of Cu occurred in BC. This was highly consistent with the DGT-profiles (Figure 15, Figure 16) which revealed sharp peaks of these four metals at the base of the added layer (5-10mm below sediment surface) in BM2, and of Cu in BC. It may be interesting to note that whereas Pb, Zn and Cd was reasonably well correlated with respect to pore water vs solid phase concentration (Table 7), Cu showed no such relationship. Cu is frequently associated with organic phases and it is possible that the organic phase responsible for the redox effects in the BC treatments was also one way or another involved in the release of Cu.

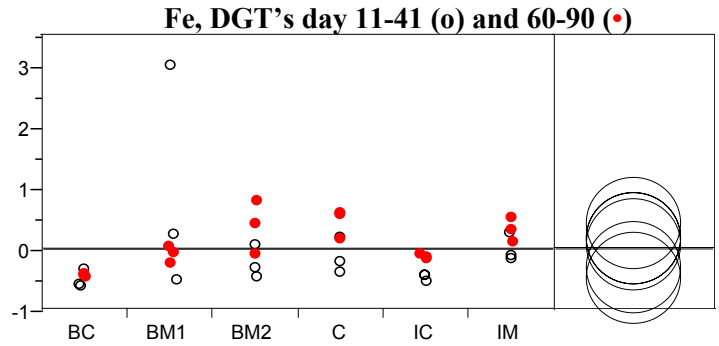

Fe DGT (µg m^{-2} h^{-1})		
Level		Mean
BM1	A	0.419
IM	A	0.154
C	A	0.153
BM2	A	0.061
IC	A	-0.302
BC	A	-0.478

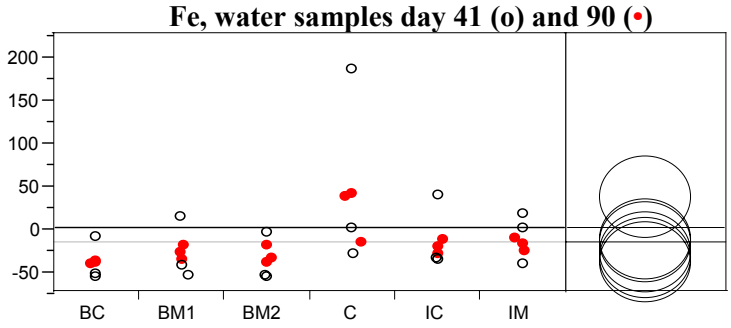

Fe HRICPMS (µg m^{-2} h^{-1})			
Level			Mean
C	A		35.2
IM	A	B	-14.2
IC	A	B	-17.3
BM1	A	B	-29.2
BM2		B	-36.1
BC		B	-40.8

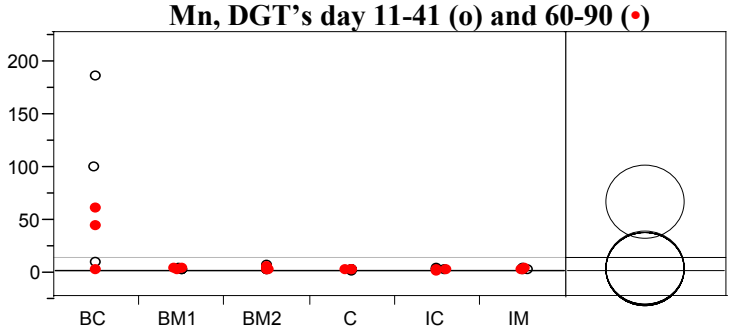

Mn DGT (µg m^{-2} h^{-1})			
Level			Mean
BC	A		65.16
BM2		B	2.04
BM1		B	1.48
IM		B	1.08
IC		B	0.55
C		B	0.49

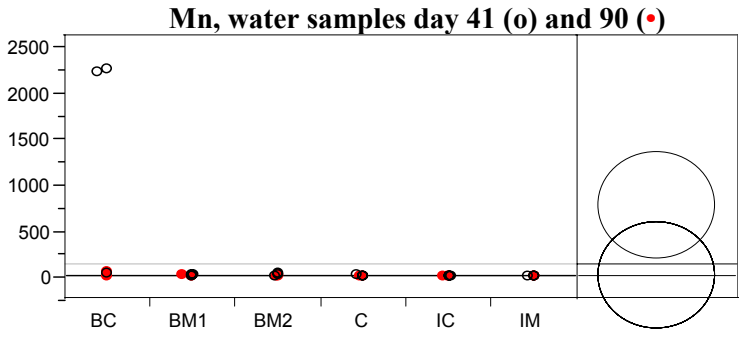

Mn HRICPMS (µg m^{-2} h^{-1})		
Level		Mean
BC	A	758.92
BM2	A	4.48
BM1	A	2.76
IM	A	-0.87
C	A	-1.81
IC	A	-2.80

Figure 14. Fluxes (µg m^{-2} h^{-1}) of iron (Fe) and manganese (Mn) determined from water samples and DGTs. Mean flux (n=6) is given in tables. Small circle overlap and letters (see text) show significant differences between treatments (ANOVA analyses, Tukey Kramer, α=0.05).

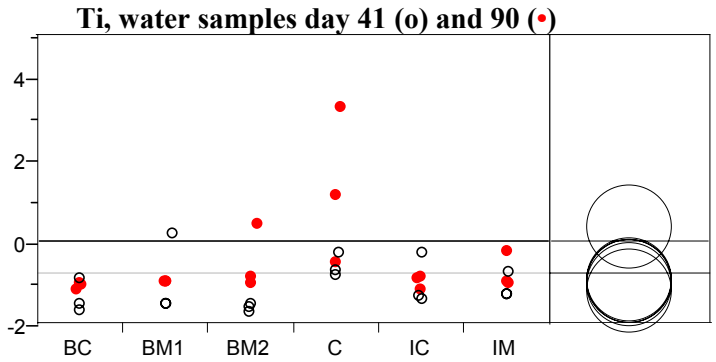

Ti HRICPMS (µg m^{-2} h^{-1})				
Level				Mean
C	A			0.359
IM	A	B		-0.919
BM1	A	B		-0.959
IC	A	B		-0.978
BM2	A	B		-1.043
BC		B		-1.216

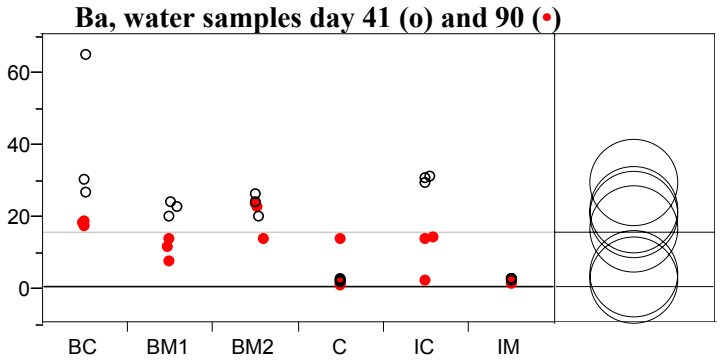

Ba HRICPMS (µg m^{-2} h^{-1})				
Level				Mean
BC	A			28.92
BM2	A			21.26
IC	A	B		19.84
BM1	A	B	C	16.15
C		B	C	3.36
IM			C	1.70

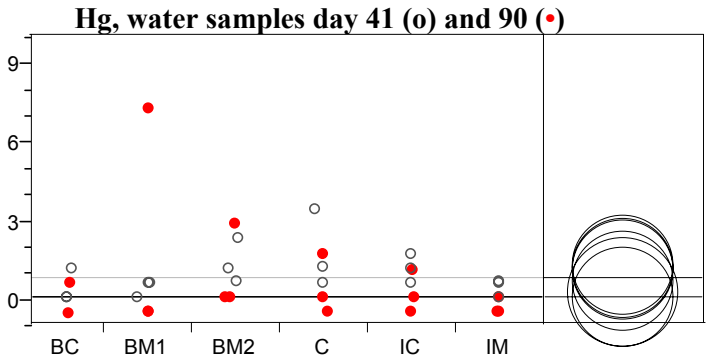

Hg (µg m^{-2} h^{-1})		
Level		Mean
BM1	A	1.204
BM2	A	1.134
C	A	1.038
IC	A	0.638
BC	A	0.219
IM	A	0.010

Figure 15. Fluxes (µg m^{-2} h^{-1}) of titanium (Ti), barium (Ba) and mercury (Hg). Mean flux (n=6) is given in tables. Small circle overlap and letters (see text) show significant differences between treatments (ANOVA analyses, Tukey Kramer, α=0.05).

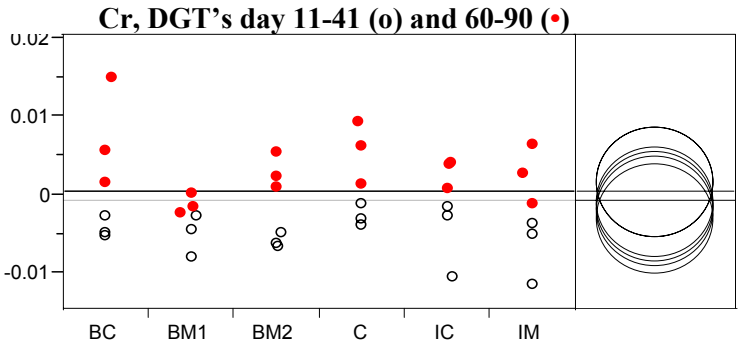

Cr DGT (µg m^{-2} h^{-1})		
Level		Mean
BC	A	0.0012
C	A	0.0012
IC	A	-0.0014
BM2	A	-0.0018
IM	A	-0.0024
BM1	A	-0.0035

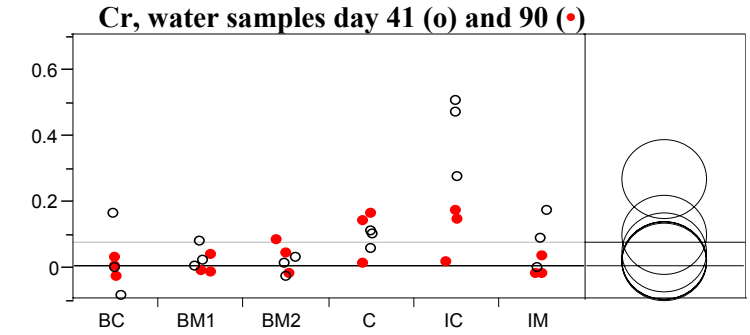

Cr HRICPMS (µg m^{-2} h^{-1})			
Level			Mean
IC	A		0.2612
C	A	B	0.0935
IM		B	0.0402
BM2		B	0.0165
BM1		B	0.0160
BC		B	0.0102

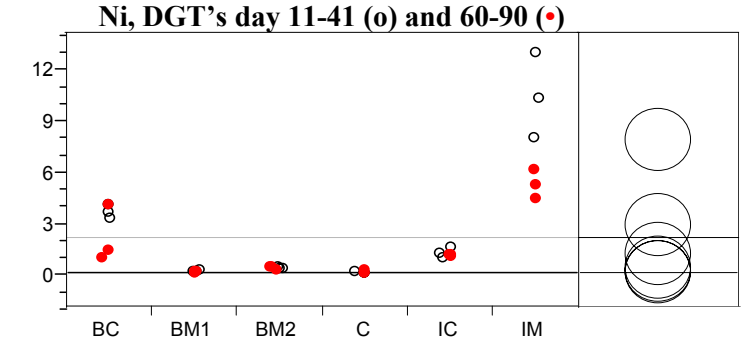

Ni DGT (µg m^{-2} h^{-1})			
Level			Mean
IM	A		7.77
BC		B	2.82
IC		B	C 1.11
BM2		B	C 0.29
BM1			C 0.10
C			C 0.04

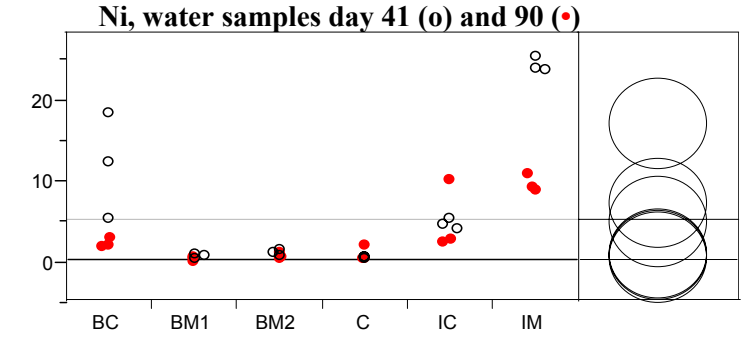

Ni HRICPMS (µg m^{-2} h^{-1})			
Level			Mean
IM	A		16.80
BC		B	7.02
IC		B	4.68
BM2		B	0.75
C		B	0.54
BM1		B	0.33

Figure 16. Fluxes (µg m^{-2} h^{-1}) of chromium (Cr) and nickel (Ni) determined from water samples and DGTs. Mean flux (n=6) is given in tables. Small circle overlap and letters (see text) show significant differences between treatments (ANOVA analyses, Tukey Kramer, α=0.05).

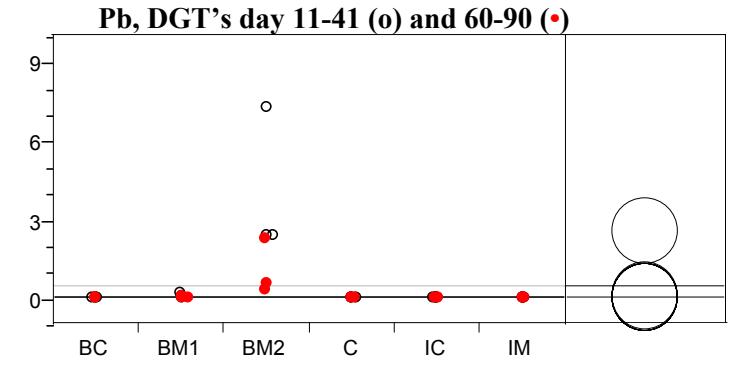

Pb DGT (µg m^{-2} h^{-1})			
Level			Mean
BM2	A		2.549
BM1		B	0.061
C		B	0.008
BC		B	0.006
IM		B	-0.000
IC		B	-0.002

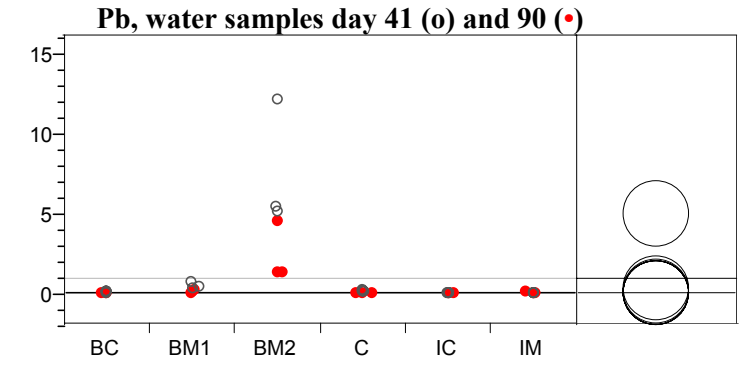

Pb Freon (µg m^{-2} h^{-1})			
Level			Mean
BM2	A		4.894
BM1		B	0.232
C		B	0.020
BC		B	-0.030
IM		B	-0.041
IC		B	-0.053

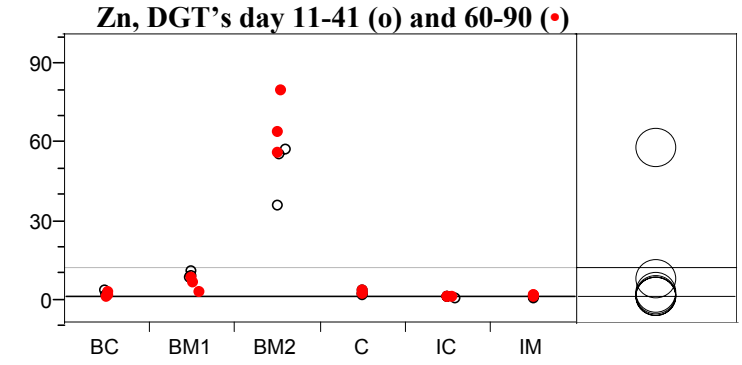

Zn DGT (µg m^{-2} h^{-1})			
Level			Mean
BM2	A		57.11
BM1		B	6.85
C		B	1.60
BC		B	0.94
IM		B	0.26
IC		B	-0.09

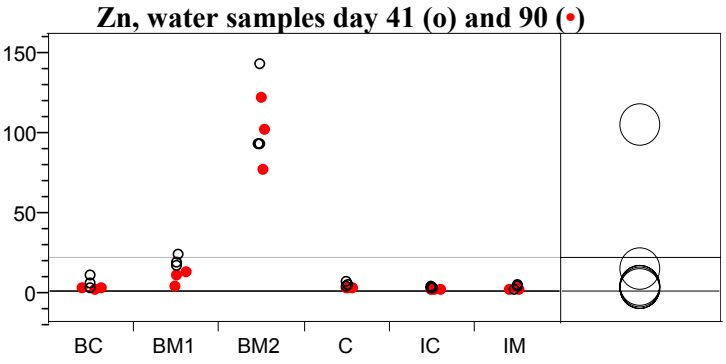

Zn HRICPMS (µg m^{-2} h^{-1})			
Level			Mean
BM2	A		103.40
BM1		B	13.29
BC		B	3.25
C		B	2.65
IM		B	1.47
IC		B	1.13

Figure 17. Fluxes (µg m^{-2} h^{-1}) of lead (Pb) and zinc (Zn) determined from water samples and DGTs. Mean flux (n=6) is given in tables. Small circle overlap and letters (see text) show significant differences between treatments (ANOVA analyses, Tukey Kramer, α=0.05).

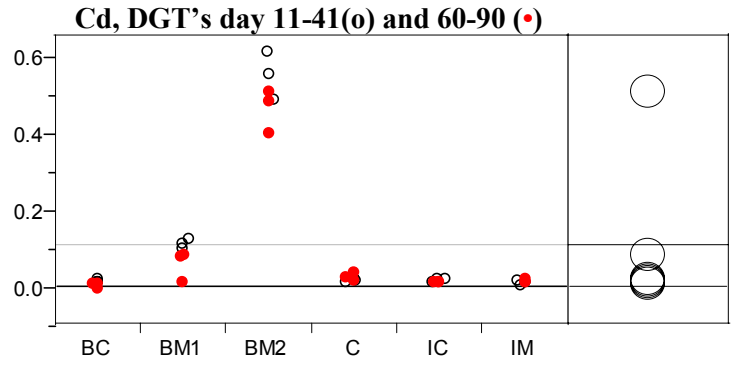

Cd DGT (µg m^{-2} h^{-1})			
Level			Mean
BM2	A		0.506
BM1		B	0.083
C		C	0.020
IC		C	0.013
IM		C	0.010
BC		C	0.008

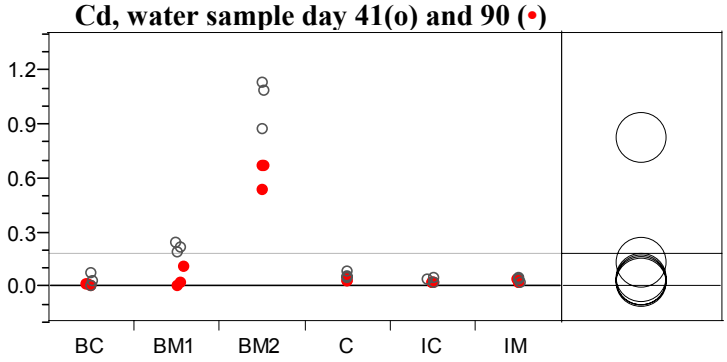

Cd Freon (µg m^{-2} h^{-1})			
Level			Mean
BM2	A		0.823
BM1		B	0.128
C		B	0.043
IM		B	0.029
IC		B	0.027
BC		B	0.019

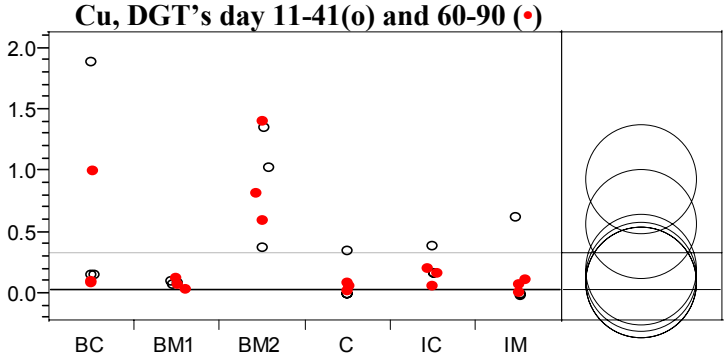

Cu DGT (µg m^{-2} h^{-1})			
Level			Mean
BM2	A		0.900
BC	A	B	0.534
IC		B	0.162
IM		B	0.103
C		B	0.058
BM1		B	0.053

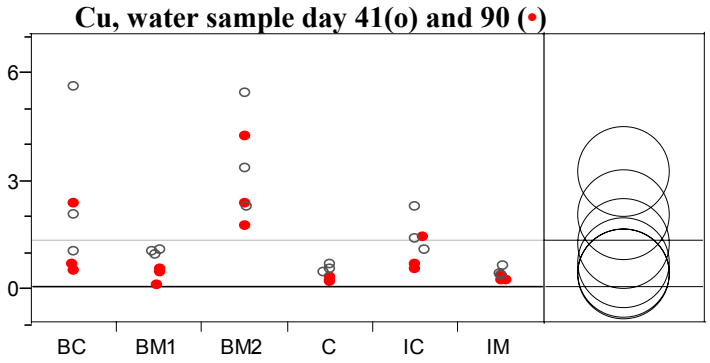

Cu Freon (µg m^{-2} h^{-1})			
Level			Mean
BM2	A		3.180
BC	A	B	1.980
IC		B	1.181
BM1		B	0.635
C		B	0.352
IM		B	0.324

Figure 18. Fluxes (µg m^{-2} h^{-1}) of cadmium (Cd) and copper (Cu) determined from water samples and DGTs. Mean flux (n=6) is given in tables. Small circle overlap and letters (see text) show significant differences between treatments (ANOVA analyses, Tukey Kramer, α=0.05).

3.4 Cellular energy allocation (CEA)

In the present study, pooled samples of *Nuculoma tenuis* were analyzed for lipid, protein and carbohydrate contents (Figure 19), as well as the energy consumption through the electron transport system (Figure 20). Due to various circumstances, one of which may have been the general depletion of the experimental communities in the two cuttings treatments, the tissue samples obtained were insufficient for analyses of the BC-treatment and only one replicate could be analysed for the IC-treatment.

The remaining samples revealed no obvious differences between treatments. Two of the samples (BM1 and IM) showed large variations in both energy stored and energy consumed. The IC sample, for which adverse health effects might have been expected, showed low concentration of carbohydrates, but total energy consumption was very similar to that of the other treatments and to control.

Despite few replicates, the data indicate that the weight material treatments had no negative physiological effects on the sediment-dwelling bivalve *Nuculoma tenuis*.

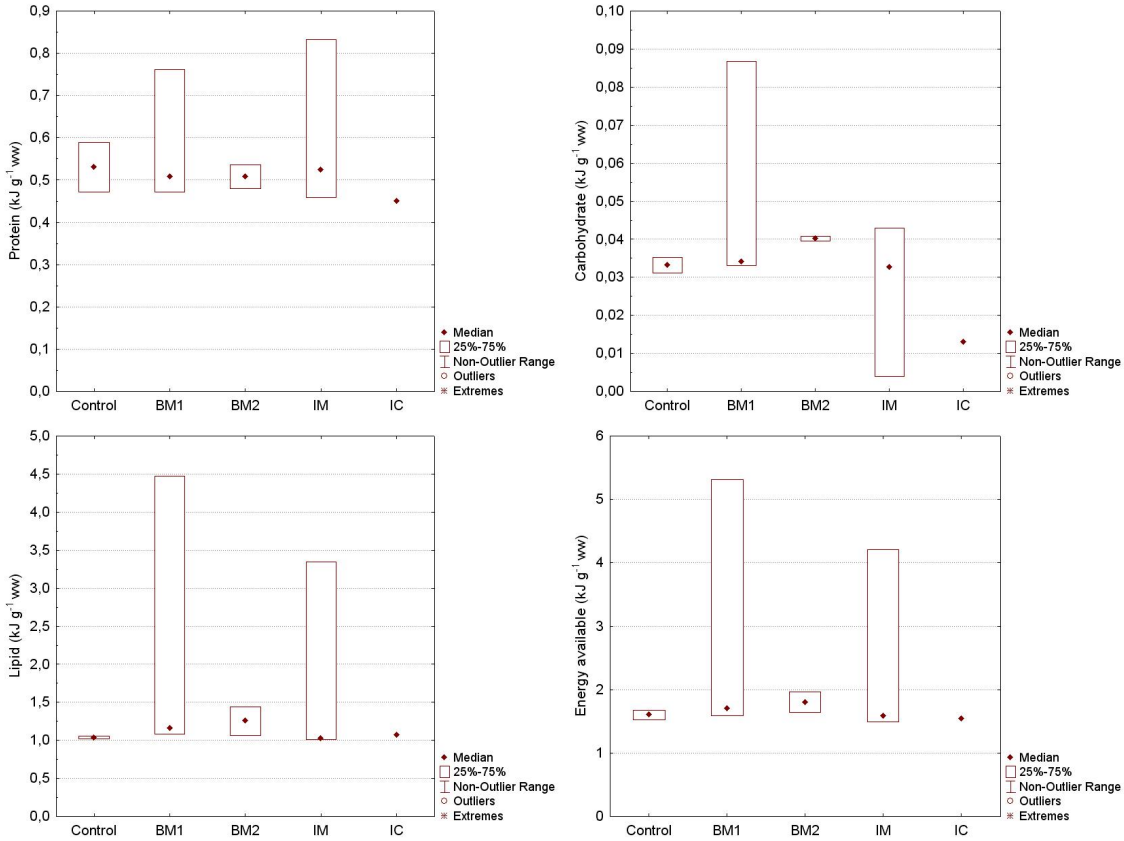

Figure 19. Box-plots of protein, carbohydrate, lipid and total energy available for *Nuculoma tenuis* held in sediment receiving the different treatments. Median and quartiles are shown. BM1; Barite minerals type 1, BM2; Barite minerals type 2, IM; Ilmenite minerals, IC; Ilmenite cuttings. N=2 for Control and BM2, n=3 for IM and BM1, n=1 for IC.

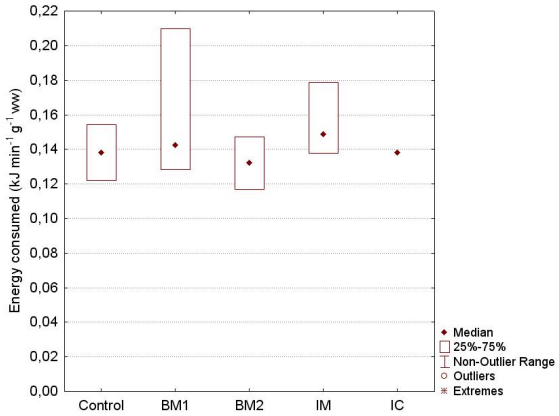

Figure 20. Box-plot of total energy consumed for *Nuculoma tenuis* held in sediment receiving the different treatments. Median and 25-75% quartiles are shown. BM1; Barite minerals type 1, BM2; Barite minerals type 2, IM; Ilmenite minerals, IC; Ilmenite cuttings. N=2 for Control and BM2, n=3 for IM and BM1, n=1 for IC.

3.5 Benthic fauna

3.5.1 Abundance data

The univariate parameters of the benthic fauna are presented in Table 9, Table 10 and Figure 21. The two cuttings treatments had clearly reduced numbers of taxa and individuals compared to the other treatments, and the largest reduction was found in the boxes treated with barite cuttings.

Table 9. Overview of number of taxa (S), number of individuals (N) and Shannon-Wiener diversity (H') in the various boxes, sorted pr. treatment, in the mesocosm experiment. Classification according to Norwegian quality criteria for fjord and coastal environments (Molvær et al., 1997).

	S	N	H'	Classification
C-3	15	62	3,2	Good
C-6	14	63	2,9	Fair
C-14	11	55	2,4	Fair
IM-7	18	95	3,0	Good
IM-12	13	75	3,0	Good
IM-15	15	75	3,0	Good
BM1-2	16	64	3,1	Good
BM1-11	19	63	3,2	Good
BM1-17	18	68	3,4	Good
BM2-5	14	83	2,6	Fair
BM2-10	10	30	2,5	Fair
BM2-19	11	56	2,4	Fair
IC-4	4	13	1,4	Bad
IC-8	4	23	1,3	Bad
IC-13	4	21	1,1	Bad
BC-1	4	4	2	Bad*
BC-9	1	4	0	Very bad
BC-16	2	9	0,5	Very bad

*H' = 2,0 is at the boundary between class iii and iv, but low numbers of species and individuals justifies class iv "bad" for this box.

Table 10. Statistical analyses (ANOVA, Tukey comparison, α=0.05) of univariate macrobenthic data. Treatments are ranked according to mean result. Treatments connected by same letter are not signicantly different.

Species (S)				Individuals (N)				Diversity (H')					
Treatment			Mean	Treatment			Mean	Treatment			Mean	Classification	
BM1	A		17.7	IM	A		81.7	BM1	A		3.23	II	Good
IM	A	B	15.3	BM1	A		65.0	IM	A		3.00	II	Good
C	A	B	13.3	C	A		60.0	C	A		2.83	III	Fair
BM2		B	11.7	BM2	A		56.3	BM2	A	B	2.50	III	Fair
IC		C	4.0	IC		B	19.0	IC		B C	1.27	IV	Bad
BC		C	2.3	BC		B	5.7	BC		C	0.83	V	Very bad

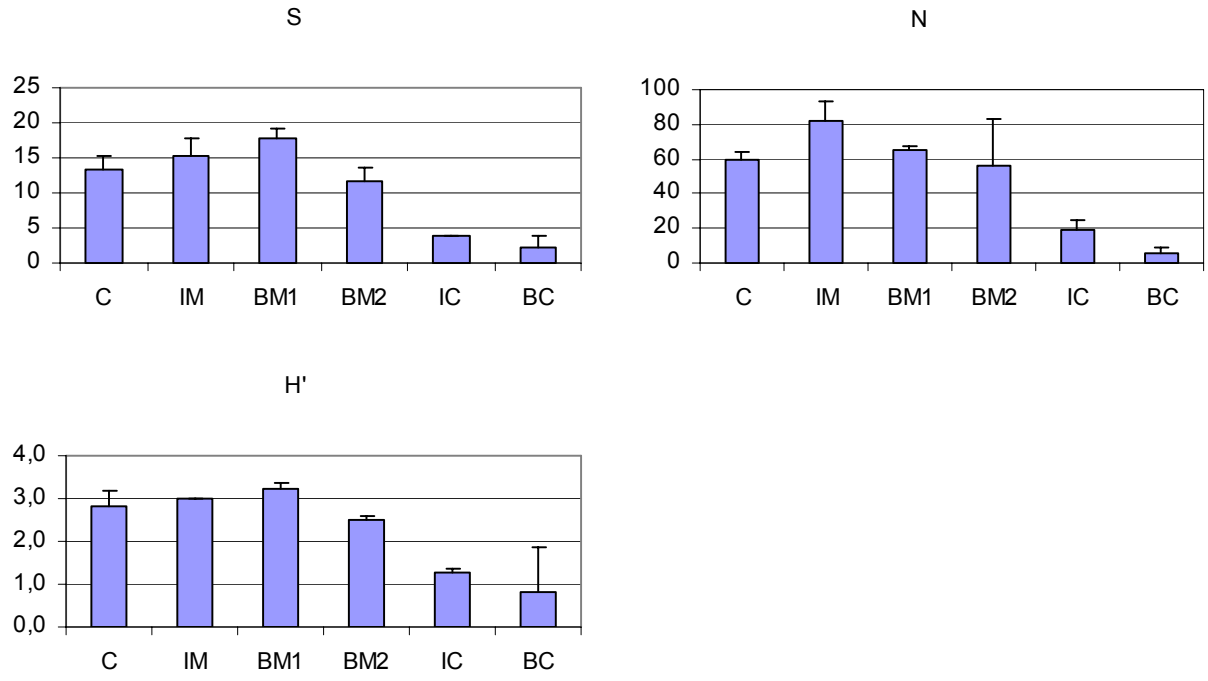

Figure 21. Mean number of taxa, number of individuals, Shannon-Wiener diversity (H') and evenness (J') in the various treatments in the mesocosm experiment, with one standard deviation.

Statistical analyses confirmed that the cuttings treatments (IC and BC) were significantly ($p<0.05$) different from C, IM and BM1 with respect to S, N and H (Table 10). BM2 ranked between control and cuttings treatments with regard to all three parameters, but none of them were significantly different from control.

Similarities in faunal structure between the samples are shown as a cluster-diagram in Figure 22 and MDS ordination in Figure 23. The cluster-analysis separated three groups of samples at a similarity of approximately 30%. The first group contained box BC-9 only. The reason for this is that this box only contained one species (the polychaete *Goniada maculata*). The second group contained all of the remaining cuttings treatments. The third group contained all control and mineral treatments. In the group containing the control and mineral treatments, two of the boxes with barite mineral 2 (BM2-10 and BM2-19) were separated from the other boxes at a similarity of 40%. The same three main groups of boxes were identified in the MDS-plot. Here it is also evident that the boxes BM2-10 and BM2-19 to some extent had a different faunal composition compared to the control boxes and the other boxes with mineral additions. Thus, the results from the multivariate analyses agreed well with the main conclusion from the univariate analyses, i.e. that the two cuttings treatments strongly affected the fauna. However, these analyses also indicate that barite mineral 2 affected the fauna in two of the respective boxes.

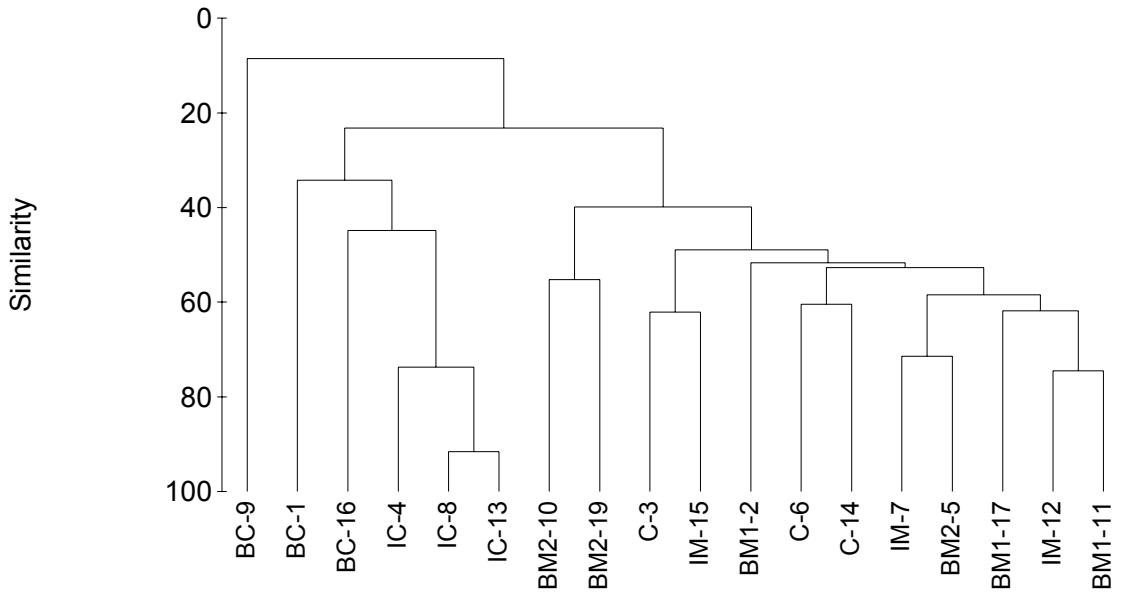

Figure 22. Cluster-analysis of the boxes in the mesocosm experiment.

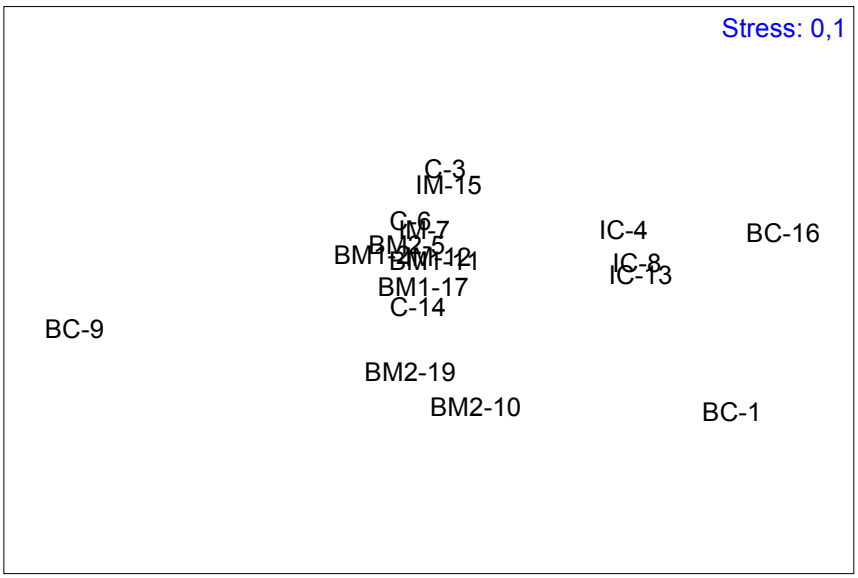

Figure 23. MDS-ordination of the boxes in the mesocosm experiment, shown as a 2-D plot.

The most abundant species in each treatment are presented in Table 11. In the control boxes and the treatments with ilmenite mineral and barite mineral 1 the bivalve *Nuculoma tenuis* and the brittle star *Amphiura filiformis* were the most abundant species. *N. tenuis* lives as a subsurface deposit feeder in the upper 2-3 cm of the sediment, while *A. filiformis* has a flexible feeding mode, and may live both as a suspension feeder, surface deposit feeder and a carnivore/omnivore depending on the local environmental conditions like e.g. the flow rate. It is usually buried in the sediment, with only its arms above the surface in order to feed and to clean and ventilate its semipermanent burrow. The abundance of *N. tenuis* was strongly reduced in the treatment with barite cuttings, while this not appeared to be the case for the ilmenite cuttings treatment. *A. filiformis* was absent from both these treatments, and also appeared to be affected by the barite mineral 2 treatment. Here it should be noted that *A. filiformis* was completely absent from two of the boxes with barite mineral 2 (BM2-10 and BM2-19), while the abundance in the last box (BM2-5) was similar to the abundance in the control and the other mineral treatments (see 5.Appendix B.).

For some reason, all three boxes with ilmenite mineral had a high abundance of the polychaete *Heteromastus filiformis* compared to the other boxes. This species lives as a subsurface deposit feeder and is well-known for being tolerant towards disturbances. Its high abundance in the ilmenite mineral treatment is assumed to be incidental and not a result of different mortality in the various treatments.

Table 11. Mean abundance of most dominating taxa in each treatment in the mesocosm experiment (0.1 m^2). Only taxa having mean abundance ≥ 1/box is included in control and mineral treatments. All taxa are included in cuttings treatments (IC and BC).

	C		IM		BM1
Nuculoma tenuis	23,67	Nuculoma tenuis	24,00	Amphiura filiformis	14,67
Amphiura filiformis	11,33	Amphiura filiformis	18,00	Nuculoma tenuis	13,67
Thyasira flexuosa	4,67	Heteromastus filiformis	13,33	Anobothrus gracilis	7,33
Nemertinea indet	3,00	Nemertinea indet	3,67	Thyasira flexuosa	5,00
Leptosynapta sp	3,00	Polycirrus plumosus	3,67	Maldane sarsi	4,00
Goniada maculata	2,33	Thyasira flexuosa	3,00	Goniada maculata	3,00
Heteromastus filiformis	1,33	Anobothrus gracilis	2,67	Amphiura chiajei	2,67
Anobothrus gracilis	1,33	Goniada maculata	2,33	Echinocardium cordatum	2,00
Echinocardium cordatum	1,33	Amphiura chiajei	1,67	Typosyllis cornuta	1,33
Diplocirrus glaucus	1,00	Mediomastus fragilis	1,33	Nemertinea indet	1,00
				Pholoe minuta	1,00
				Polycirrus plumosus	1,00
				Sabellidae indet	1,00
	BM2		IC		BC
Nuculoma tenuis	25,67	Nuculoma tenuis	13,67	Heteromastus filiformis	2,67
Nemertinea indet	7,00	Heteromastus filiformis	2,00	Goniada maculata	1,33
Amphiura filiformis	4,33	Thyasira flexuosa	1,67	Maldane sarsi	0,67
Maldane sarsi	3,33	Maldane sarsi	1,33	Spiochaetopterus typicus	0,33
Polycirrus plumosus	3,00	Cerianthus lloydi	0,33	Nuculoma tenuis	0,33
Lumbrineris sp	1,67			Corbula gibba	0,33
Goniada maculata	1,33				
Echinocardium cordatum	1,33				
Anobothrus gracilis	1,00				
Thyasira flexuosa	1,00				
Priapulus caudatus	1,00				
Amphiura chiajei	1,00				

3.5.2 Biomass data

The main groups of fauna were weighed, and the results shown in Figure 24. It is evident that the biomass data supports the results from the abundance data, i.e. that the treatments with cuttings strongly affected the fauna, and that the most severe effect was found for the barite cuttings treatment. The sea urchin *Echinocardium cordatum* made up a very large part of the biomass where it was present, and in box BM2-10 the large bivalve *Arctica islandica* made up the major part of the biomass. Dead animals were not included in the fauna-analyses, but remnants of dead animals were recorded during final sampling. In addition to those reported in the species list, empty tests of a large sea urchin (probably *E. cordatum*) were recorded in BM1-2 (3 individuals), BM2-5 (1 individual), IC-4 (2 individuals), IC-13 (1 individual), IM-15 (2 individuals), BM1-11 (1 individuals). Thus, *E. cordatum* appeared to have been absent in 7 boxes throughout the experiment. We can think of nothing but random factors to explain the fact that three of these were treated with barite cuttings.

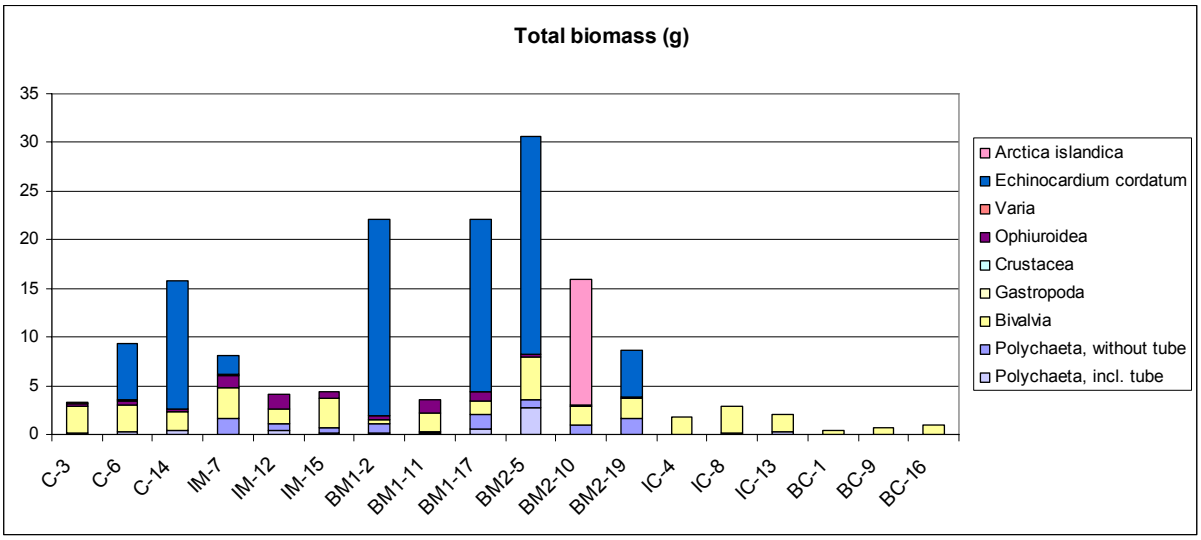

Figure 24. Biomass measurement of main groups of fauna in each box.

3.5.3 Discussion, fauna

Both the univariate and multivariate analyses of the abundance data and the biomass data showed a clear effect of added cuttings on the fauna. The most severe effect was found in the barite cuttings treatment in which almost no species survived. Also in the boxes treated with ilmenite cuttings, very few species and individuals were present at the end of the experiment. As discussed above, the treatments with cuttings showed a reduced thickness of oxygenated sediment and lowered redox potentials. Thus, hypoxia is concluded to be the main responsible factor for the impoverished communities in the cuttings treatments. The fact that no large bioturbators, neither alive nor dead, were found in any one of the three barite cuttings treatments may suggest that, incidentally, these three boxes were devoid of large bioturbators from the start of the experiment. Large individuals of *E. cordatum* are important bioturbators providing mechanical mixing within the top layer of the sediment. This activity may contribute to the maintenance of the redox cline at 2-3 cm depth (Figure

6) and it cannot be ruled out that the lack of such species in the boxes treated with barite cuttings have contributed to the extreme depletion of the communities in these boxes.

The three boxes with barite mineral 2 were variable with respect to faunal composition. In the multivariate analyses one of the boxes (BM2-5) was grouped together with the other boxes in the control and mineral treatments, while the two other boxes (BM2-10 and BM2-19) formed a separate group. This grouping is assumed to a large degree to arise from the fact that the brittle star *Amphiura filiformis* was completely absent from the boxes BM2-10 and BM2-19. In addition the number of species and individuals were lower in BM2-10 and BM2-19 than in BM2-5. In the BM2 treatment class II concentrations of copper, lead and zinc were recorded (see chapter 3.1) and the release of cadmium, lead, zinc and copper from this treatment was high compared to the other treatments (see chapter 3.3). However, if one or more of these metals have affected *A. filiformis*, the concentrations and/or fluxes should have been higher in the boxes BM2-10 and BM2-19 than in box BM2-5. The pore water concentrations of all metals were higher in BM2-5 than in the two other replicates, but, higher fluxes of copper and zinc were recorded in BM2-10 and BM2-19 compared to BM2-5. The fluxes were measured much more extensively than the pore water concentrations measured only once at the end of the study. Also the flux is probably a better measure of the availability of metals for uptake in organisms than the pore water concentration. Thus, the more disturbed community and the higher fluxes of Cu and Zn in BM2-10 and BM2-19 compared to BM2-5, seemed to indicate a potential effect of copper and/or zinc on macrobenthic species. In particular *A. filiformis* may appear vulnerable.

As far as we know, no data exist on the relationship between fluxes of metals and the mortality of benthic species. However, Cu is generally known to be toxic to marine species (hence it's use in antifouling paints) and from a toxicity study it has been concluded that *A. filiformis* is moderately sensitive to copper (Bowmer et al., 1986). Based on field data, Rygg (1985) classified this species as non-tolerant towards copper, as it was only occasionally found at stations with sediment copper concentrations above 200 ppm. Thus, the observed effects on the fauna in BM2 appeared to yield one of very rare evidences on metal toxicity on marine, benthic species. However, clear and significant depletion of benthic communities were only found to result from hypoxia in the cuttings treatments.

4. Conclusions

- One of the two barite samples tested (BM2) was class iii (markedly polluted) with cadmium, copper, lead and zinc and released more of these metals to the overlying seawater than the other experimental treatments and untreated control sediments.
- Multivariate statistical analyses indicated a relationship between the higher metal mobility in BM2 and the composition of the macrobenthic community.
- Ilmenite was class iii (markedly polluted) with nickel and chromium. Nickel was released to the overlying seawater at higher rates than it was released from untreated control sediments.
- In all test products, the concentration of mercury was lower than in the control sediments and the release of mercury from sediments to water was higher from control sediments than from sediments treated with cuttings or weight minerals.
- Compared to untreated control sediments and sediments treated with weight minerals only, water-based cuttings affected sediment chemistry and biota by:
    - Less oxygen (O_2), more hydrogen sulphide (H_2S) and lower redox potentials
    - Reduced number of macrobenthic species and indivduals and reduced biodiversity.
- Biological analyses showed
    - no significant difference between sediments treated with barite and ilmenite minerals, and
    - no significant difference between sediments treated with barite and ilmenite cuttings.
- Reduced number of species in sediments treated with high metal barite (BM2) compared to the low metal barite (BM1) indicated that metal release may affect biodiversity in marine sediments when oxygen conditions are not impoverished by mud or cuttings components.
- If barite used in the production of waterbased muds, which later become discharged from off-shore drilling operations, is substituted either with ilmenite or with barite with less trace metal impurities than BM2, the release of cadmium, copper, lead and zinc from cuttings discharged in the off-shore environment may be reduced.
- The concentration of mercury were lower in all test materials than in the control sediment. The highest release of Hg was observed from the two barite mineral treatments and the lowest release was from ilmenite minerals. However, no significant difference were found between Hg fluxes from any treatments.

5. References

Bågander, L.E. and L.Niemistö, 1978. An evaluation of the use of redox measurements for characterising recent sediments. Estuarine Coastal Mar. Sci., 6, 127-134.

Bligh EG, Dyer WJ (1959) A rapid method of total lipid extraction and purification. Canadian Journal of Biochemistry and Physiology 37: 911-917

Bowmer, T. Boelens, R.G.V., Keegan, B.F. and O'Neill, J., 1986. The use of marine benthic "key" species in ecotoxicological testing: *Amphiura filiformis* (O.F. Müller) (Echinodermata: Ophiuroidea). Aquatic Toxicology 8: 93-109.

Daan, R., Mulder, M., Van Leeuwen, A., 1994. Differential sensitivity of macrozoobenthic species to discharges of oil-contaminated drill cuttings in the North Sea. Netherlands Journal of Sea Research 33 (1): 113-127.

Davison, W. and H.Zhang, 1994. In situ speciation measurements of trace components in natural waters using thin-film gels. *Nature*, 367, 546-548.

Davison W, Fones GR and Grime GW, 1997. Dissolved metals in surface sediment and a microbial mat at 100-mu m resolution. *Nature,* 387 (6636): 885-888.

DeCoen W, Janssen C (1997) The use of biomarkers in *Daphnia Magna* toxicity testing. IV. Cellular Energy Allocation: a new methodology to assess the energy budget of toxicant-stressed Daphnia populations. Journal of Aquatic Ecosystem Stress and Recovery 6: 43-55

Gnaiger E (1983) Appendix C Calculation of Energetic and Biochemical Equivalents of Respiratory Oxygen Consumption. In: Forstner G (ed) Polarographic Oxygen Sensors. Springer-Verlag, Berlin Heidelberg.

Harvey R, Gage JD (1995) Reproduction and recruitment of *Nuculoma tenuis* (Bivalvia: Nuculoida) from Loch Etive, Scotland. Journal of Molluscan Studies 61: 409-419

King F, Packard T (1975) Respiration and the activity of the respiratory electron transport system in marine zooplankton. Limnology and oceanography 20: 849-854

Lowry OH, Rosebrough NJ, Farr AL, Randall RJ (1951) Protein measurements with the Folin phenol reagent. Journal of Biological Chemistry 193: 265-275

Molvær J, Knutzen J, Magnusson J, Rygg B, Skei J, Sørensen J, 1997. Klassifisering av miljøkvalitet i fjorder og kystfarvann. [Classification of environmental quality in fjords and coastal waters.] Veiledning. SFT-veiledning nr. 97:03, TA-1467/1997. 36 pp. (In Norwegian).

PRIMER-E LTD, 2002. PRIMER 5 for Windows V 5.2. Plymouth, United Kingdom.

Rygg, B., 1985. Effect of sediment copper on benthic fauna. Mar. Ecol. Progr. Ser. 29: 83-89.

Schaanning, M.T., K.Hylland, D.Ø.Eriksen, T.D.Bergan, J.S.Gunnarson and J.Skei, 1997. Interactions Between Eutrophication and Contaminants: II Mobilization and Bioaccumulation of Hg and Cd from Marine Sediments. Marine Pollution Bulletin, Vol. 33, Nos 1-6, pp. 71-79.

Schaanning, M.T, Ruus, A., Bakke, T., Hylland, K., Olsgard, F., 2002. Bioavailability of metals in weight materials for drilling muds. Norsk institutt for vannforskning (NIVA). Rapport l.nr 4597-02, 36 pp.

Schaanning, M.T., Trannum, H.C. and Øxnevad, S., 2007. A mesocosm experiment on the impacts of water- and olefin-based drill cuttings on benthic communities. NIVA report SNO 5342-2007. 53 pp.

Verslycke T, Roast SD, Widdows J, Jones MB, Janssen Cr (2004) Cellular Energy Allocation and scope for growth in the estuarine mysid Neomysis integer (Crustacea: Mysidacea) following chlorpyrifos exposure: a method comparison. Journal of experimental marine biology and ecology 306: 1-16

Voets J, Talloen W, De Tender T, Van Dongen S, Covaci A, Blust R, Bervoets L (2006) Microcontaminant accumulation, physiological condition and bilateral asymmetry in zebra mussels (Dreissena polymorpha) from clean and contaminated surface waters. Aquatic Toxicology 79(3): 213-225

Widdicombe S, Austen MC (1999) Mesocosm investigation into the effects of bioturbation on the diversity and structure of a subtidal macrobenthic community. Marine Ecology Progress Series 189: 181-193

Øverås NH (2006) Cellular energy allocation in the sediment dwelling bivalves Astarte sulcata, Nuculoma tenuis and Macoma calcarea. Master of Science thesis. Department of biology, Oslo.

Appendix A. Test substances and declarations

Barite minerals type 1 (BM1)

Plastspann ca 5L,
Merket: 06.04.27-003. 420 Prøvelast "Moon Fox" 05.12.05
Innhold: ca 3 kg gulaktig mineralsk tørt materiale. Finmalt, pudder.

West Lab Services, Laboratorierapport. Analyser av tungmetaller i baryttprøve nr 2005-06088-001 tatt 05.12.2005, merket M/S "Moon Fox"-Comabar Nador, 5319 M/T. Prøve mottat (Intertek) 14.12.05, analysert januar 2006.
Resultat bl.a.: 2.4 mg Hg/kg, 98 mg Pb/kg.

Barite minerals type 2 (BM2)

Plastspann ca 5L,
Merket: 06.04.27-002. 12 Prøvelast "Wilson Riga" 9/1-06
Innhold: ca 3 kg gulaktig mineralsk tørt materiale. Finmalt, pudder.

Intertek West Lab, Laboratorierapport. Analyser av tungmetaller i baryttprøve nr 2006-01632-001 tatt 09.01.2006, merket M/V "Wilson Riga"-Comabar Nador, 5711 M/T. Prøve mottat (Intertek) 25.01.06, analysert mars 2006.
Resultat bl.a.: 0.07 mg Hg/kg, 263 mg Pb/kg.

Barite cuttings (BC)

Plastspann ca 5L,
Merket: Glydrill/Baritt Kaks Well 33/12-N-3H 18/5-06 24:00 Depth 2160 T?D 2021
Innhold: 3,3 kg grått, fuktig, sedimentlignende materiale.

Ilmenite minerals (IM)

Plastbeholder fra Titania AS, 4380 Hauge i Dalane, ca 1L
Merket: 2006106-1 Vektmatr.
Innhold: ca 3 kg svart mineralsk tørt materiale. Finmalt, som pudder.

Ilmenite cuttings (IC)

2 bokser
Merket: Glydril/Ilmenitt kaks (Snøhvit)
Innehold: ca 8 kg fuktig, svart kaks. Finmalt, klumper.

Appendix B. Species list

Group	Family	Species	1	2	3	4	5	6	7	8	9	10	11	12	13	14	15	16	17	19
Anthozoa	Cerianthidae	Cerianthus lloydi		1		1	2		1				1				1			
Nemertinea		Nemertinea indet		1	7		2	2	3				2	1			7			19
Polychaeta	Aphroditidae	Aphrodita aculeata					1		1											
Polychaeta	Sigalionidae	Pholoe minuta							1				2						1	
Polychaeta	Syllidae	Typosyllis cornuta		2													2		2	
Polychaeta	Nereidae	Eunereis longissimus												1		1				
Polychaeta	Nephtyidae	Nephtys cf. hombergii											1				2			
Polychaeta	Nephtyidae	Nephtys hombergii						2	1			2								
Polychaeta	Glyceridae	Glycera alba			1								1	1		1	1		1	
Polychaeta	Goniadidae	Goniada maculata		2	2		1	2	2		4	2	1	4		3	1		6	1
Polychaeta	Lumbrineridae	Lumbrineris sp										1				1				4
Polychaeta	Apistobranchidae	Apistobranchus tullbergi			1															
Polychaeta	Spionidae	Prionospio cirrifera		1																
Polychaeta	Spionidae	Prionospio fallax			1											1				
Polychaeta	Chaetopteridae	Spiochaetopterus typicus	1																	
Polychaeta	Cirratulidae	Chaetozone setosa											1							
Polychaeta	Flabelligeridae	Brada villosa							1										1	
Polychaeta	Flabelligeridae	Diplocirrus glaucus						2								1				
Polychaeta	Scalibregmidae	Polyphysia crassa					1		1				1	1					1	
Polychaeta	Scalibregmidae	Scalibregma inflatum															1			2
Polychaeta	Capitellidae	Heteromastus filiformis			3	1		1	13	4			2	14	1		13	8		
Polychaeta	Capitellidae	Mediomastus fragilis			2												4			
Polychaeta	Maldanidae	Maldane sarsi	1				8			1		2	1		3			1	11	
Polychaeta	Oweniidae	Myriochele oculata			1															
Polychaeta	Pectinariidae	Pectinaria auricoma			1														1	
Polychaeta	Ampharetidae	Anobothrus gracilis		20				2	4			2	1	4		2			1	1
Polychaeta	Ampharetidae	Melinna cristata					2													
Polychaeta	Terebellidae	Amaeana trilobata															1			
Polychaeta	Terebellidae	Polycirrus plumosus			2		3		4			3	1	3			4		2	3
Polychaeta	Trichobranchidae	Trichobranchus roseus											1	1						
Polychaeta	Sabellidae	Sabellidae indet		2															1	
Ologochaeta		Oligochaeta indet																	1	
Opistobranchia	Scaphandridae	Cylichna alba						1												1
Caudofoveata		Caudofoveata indet		2			1	1	1											
Bivalvia	Nuculidae	Nuculoma tenuis	1	5	21	9	41	23	29	16		15	19	19	16	27	24		17	21
Bivalvia	Nuculanidae	Nuculana pernula																	1	
Bivalvia	Thyasiridae	Thyasira flexuosa		6	3	2	3	6	3	2			5	5	1	5	1		4	
Bivalvia	Lasaeidae	Montacuta ferruginosa		1																
Bivalvia	Scrobiculariidae	Abra nitida						2												
Bivalvia	Arcticidae	Arctica islandica										1								
Bivalvia	Corbulidae	Corbula gibba	1	1								1								
Pycnogonida		Pycnogonida indet											1							
Ostracoda	Cypridinidae	Philomedes lilljeborgi		1													1			
Priapulida		Priapulus caudatus					2		1											1
Ophiuroidea	Amphiuridae	Amphiura chiajei		2								1	4	5					2	2

Ophiuroidea	Amphiuridae	Amphiura filiformis		15	9		13	15	26		17	16		10	12		12									
Echinoidea	Loveniidae	Echinocardium cordatum		2			3	1	1		1			3			3	1								
Holothuroidea	Synaptidae	Labidoplax buski			2																					
Holothuroidea	Synaptidae	Leptosynapta sp			6			3	2																	

Appendix C. PRIMER results

Similarity

Create triangular similarity/distance matrix

Worksheet

File: H:\26152 BARIL\artsdata\artliste_stat.xls
Sample selection: All
Variable selection: All

Parameters

Analyse between: Samples
Similarity measure: Bray Curtis
Standardise: No
Transform: Fourth root

Outputs

Worksheet: Sheet2

CLUSTER

Hierarchical Cluster analysis

Similarity Matrix

File: Sheet2
Data type: Similarities
Sample selection: All

Parameters

Cluster mode: Group average
Use data ranks: No

Samples

 1 C-3
 2 C-6
 3 C-14
 4 IM-7
 5 IM-12
 6 IM-15
 7 BM1-2
 8 BM1-11
 9 BM1-17
10 BM2-5
11 BM2-10
12 BM2-19
13 IC-4
14 IC-8
15 IC-13
16 BC-1
17 BC-9
18 BC-16

Combining

14+15 -> 19 at 91,58
5+8 -> 20 at 74,53

13+19 -> 21 at 73,71
4+10 -> 22 at 71,4
1+6 -> 23 at 62,12
9+20 -> 24 at 61,79
2+3 -> 25 at 60,48
22+24 -> 26 at 58,43
11+12 -> 27 at 55,23
25+26 -> 28 at 52,69
7+28 -> 29 at 51,66
23+29 -> 30 at 48,94
18+21 -> 31 at 44,87
27+30 -> 32 at 39,89
16+31 -> 33 at 34,23
32+33 -> 34 at 23,25
17+34 -> 35 at 8,53

Outputs

Plot: Plot1

MDS

Non-metric Multi-Dimensional Scaling

Similarity Matrix

File: Sheet2
Data type: Similarities
Sample selection: All

Best 3-d configuration (Stress: 0,07)

Sample	1	2	3
C-3	0,25	0,50	0,38
C-6	0,40	0,18	0,22
C-14	0,34	-0,11	0,33
IM-7	0,36	0,31	-0,14
IM-12	0,28	0,04	-0,02
IM-15	0,23	0,60	0,02
BM1-2	0,46	0,08	-0,58
BM1-11	0,26	0,07	-0,14
BM1-17	0,32	-0,15	-0,32
BM2-5	0,27	0,25	-0,38
BM2-10	0,00	-0,82	0,08
BM2-19	0,47	-0,64	0,06
IC-4	-0,87	0,32	-0,28
IC-8	-0,94	0,10	0,09
IC-13	-0,97	0,03	0,04
BC-1	-1,45	-0,80	-0,11
BC-9	2,27	-0,23	0,31
BC-16	-1,66	0,26	0,45

Best 2-d configuration (Stress: 0,1)

Sample	1	2
C-3	-0,19	0,63
C-6	-0,40	0,32
C-14	-0,35	-0,19
IM-7	-0,32	0,26
IM-12	-0,23	0,10
IM-15	-0,17	0,53
BM1-2	-0,62	0,11
BM1-11	-0,26	0,08
BM1-17	-0,32	-0,07
BM2-5	-0,42	0,17
BM2-10	-0,01	-0,78
BM2-19	-0,40	-0,58

IC-4	0,87	0,26
IC-8	0,94	0,06
IC-13	0,96	0,00
BC-1	1,51	-0,81
BC-9	-2,39	-0,32
BC-16	1,81	0,24

STRESS VALUES

Repeat	3D		2D
1	0,08		0,11
2	0,08		0,10
3	0,08		0,10
4	0,08		0,10
5	0,08		0,12
6	0,07		0,10
7	0,09		0,12
8	0,08		0,10
9	0,08		0,14
10	0,08		0,12
11	0,09		0,10
12	0,07		0,10
13	0,07		0,10
14	0,07		0,10
15	0,10		0,12
16	0,08		0,12
17	0,07		0,10
18	0,08		0,10
19	0,08		0,10
20	0,07		0,10
21	0,09		0,10
22	0,09		0,10
23	0,08		0,10
24	0,07		0,10
25	0,08		0,10
26	0,07		0,10
27	0,07		0,10
28	0,08		0,10
29	0,07		0,12
30	0,07		0,10
31	0,08		0,10
32	0,08		0,10
33	0,08		0,12
34	0,08		0,10
35	0,09		0,10
36	0,08		0,10
37	0,07		0,10
38	0,07		0,10
39	0,09		0,10
40	0,08		0,10
41	0,07		0,10
42	0,08		0,10
43	0,09		0,11
44	0,08		0,10
45	0,09		0,12
46	0,09		0,11
47	0,07		0,10
48	0,08		0,11
49	0,07		0,11
50	0,08		0,13
51	0,08		0,10
52	0,09		0,11
53	0,07	**	0,10
54	0,08		0,10
55	0,08		0,10
56	0,08		0,10
57	0,08	**	0,10

```
    58  0,09       0,13
    59  0,08 **    0,10
    60  0,08       0,10
    61  0,09       0,10
    62  0,08       0,11
    63  0,07       0,10
    64  0,08       0,10
    65  0,08       0,13
    66  0,09       0,11
    67  0,09       0,11
    68  0,07       0,10
    69  0,07       0,10
    70  0,07       0,10
    71  0,08       0,10
    72  0,08       0,14
    73  0,07       0,10
    74  0,07       0,10
    75  0,08       0,11
    76  0,08       0,12
    77  0,09       0,10
    78  0,09       0,10
    79  0,08       0,10
    80  0,08       0,12
    81  0,08       0,10
    82  0,08       0,11
    83  0,08       0,10
    84  0,08 **    0,10
    85  0,08       0,10
    86  0,08       0,10
    87  0,07       0,10
    88  0,08       0,10
    89  0,07       0,10
    90  0,07       0,11
    91  0,09       0,10
    92  0,07       0,11
    93  0,07       0,12
    94  0,08       0,10
    95  0,07       0,10
    96  0,08       0,10
    97  0,08       0,10
    98  0,07       0,10
    99  0,08       0,10
   100  0,07       0,10

** = Maximum number of iterations used

3-d : Minimum stress: 0,07 occurred 31 times
2-d : Minimum stress: 0,1 occurred 71 times
```

Outputs

Plot: Plot2